

Synthesis and Characterization of Triethylsiloxy-Substituted Alumoxanes: Their Structural Relationship to the Minerals Boehmite and Diaspore

Allen W. Apblett, Alison C. Warren, and Andrew R. Barron*

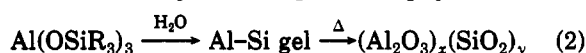
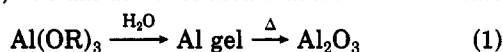
Department of Chemistry and Materials Research Laboratory, Harvard University, Cambridge, Massachusetts 02138

Received July 29, 1991. Revised Manuscript Received October 16, 1991

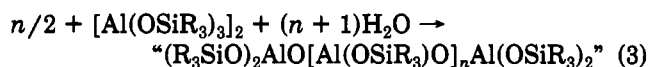
Triethylsiloxy-substituted alumoxanes, $[\text{Al}(\text{O})(\text{OH})_x(\text{OSiEt}_3)_{1-x}]_n$, have been prepared and characterized by infrared, multinuclear magnetic resonance, and X-ray photoelectron spectroscopies. Hydrolytically stable alumoxanes prepared by both solid state (1, 2) and solution (3) hydrolysis of $[\text{Al}(\text{OSiEt}_3)_3]_2$ have a high hydroxide content ($0.81 < x < 0.85$), predominantly six-coordinate aluminum, and a single terminal siloxide environment. In contrast, alumoxane 4 prepared from the reaction of methylalumoxane, $[\text{Al}(\text{O})\text{Me}]_n$, with Et_3SiOH has no hydroxide substituents, largely four-coordinate aluminum, and both bridging and terminal siloxide groups. Based on the spectroscopy of the alumoxanes 1-4, a structural model for siloxaluminum has been proposed in which a six-coordinate aluminum/oxygen core, analogous to that found in the minerals boehmite and diasporite, $[\text{Al}(\text{O})(\text{OH})]_n$, is encapsulated by end/edge groups consisting of four-coordinate aluminum atoms within a six-membered ring. It is on these four-coordinate aluminum centers that the Et_3SiO substituents are located. Confirmation of this proposed structure has been obtained by the isolation and X-ray crystallographic structural characterization of the decaaluminum cluster $\text{Al}_{10}(\text{OH})_{16}(\text{OSiEt}_3)_{14}$ (6), prepared from the thermolysis of the alumoxane 5 formed from the reaction of $[\text{Al}(\text{OSiEt}_3)_3]_2$ with 0.25 mol equiv of H_2O . The relationship between 6, the isolated hydrolytically stable alumoxanes and the minerals boehmite and diasporite are discussed. Crystal data for 6 are as follows: triclinic $P\bar{1}$ [No. 2], $a = 15.62$ (1), $b = 15.92$ (2), $c = 17.768$ (7) Å, $\alpha = 106.84$ (7), $\beta = 97.56$ (5), $\gamma = 119.33$ (6)°, $Z = 1$, $R = 0.125$, $R_w = 0.143$.

Introduction

With a combined annual production of over 30 million tons, the oxides and hydroxides of aluminum are undoubtedly among the most industrially important chemicals.¹ Their uses include precursors for the production of aluminum metal, catalysts, and absorbants; structural ceramic materials; reinforcing agents for plastics and rubbers, antacids, and binders for the pharmaceutical industry; and as low dielectric loss insulators in the electronics industry. With such a diverse range of applications, it is unsurprising that much research has been focused on developing and understanding new methods for the preparation of these materials. A common route to all of the aluminum oxides and hydroxides is via alumina gels. Sometimes referred to as gelatinous alumina, these are two-phase systems in which colloidal aluminum hydroxide, or an oxide hydroxide based material, is the predominant solid phase; the second phase being water, an organic solvent, or both. Gelatinous aluminas have traditionally been prepared by the neutralization of a concentrated aluminum salt solution;² however, the strong interactions of the freshly precipitated alumina gels with ions from the precursors solutions makes it difficult to prepare the gels in pure form.³ To avoid this complication, alumina gels may be prepared from the hydrolysis of aluminum alkoxides, $[\text{Al}(\text{OR})_3]_n$. Although this method was originally reported by Adkins in 1922,⁴ it was not until the 1970s when Teichner and co-workers⁵ reported the preparation of alumina aerogels, and Yoldas⁶ showed that transparent ceramic bodies can be obtained by the pyrolysis of suitable alumina gels, that interest increased significantly. In addition to the formation of alumina bodies from the pyrolysis of gels prepared by the hydrolysis of aluminum alkoxides (eq 1), Yoldas demonstrated that aluminum silicate



ceramics, $(\text{Al}_2\text{O}_3)_x(\text{SiO}_2)_y$, could also be prepared using related methodology (eq 2).⁷ The aluminum-silicon based gels formed on the hydrolysis of aluminum siloxides (eq 2) are clearly related to the siloxy substituted aluminum-based polymers, alumoxanes,⁸ first reported in 1958 by Andrianov (eq 3),⁹ suggesting that the "alumina gels"



prepared from aluminum alkoxides and siloxides are not colloidal aluminum hydroxides, or oxide hydroxides, but alumoxanes, i.e., organically substituted aluminum oxygen macromolecules.

In addition to their use as preceramics, alumoxane based materials also find uses as additives in paints and coatings, antiperspirants, supports for metal colloids, and catalysis. In regard to this latter area, alkyl-substituted alumoxanes, $[\text{Al}(\text{O})\text{R}]_n$, obtained from the reaction of organoaluminum compounds and water (eq 4), were extensively studied in



the 1960s as active catalysts in the polymerization of propylene oxide,¹⁰ epoxides,¹¹ butadiene,¹² and propylene.¹³

(1) Wefers, K.; Misra, C. *Oxides and Hydroxides of Aluminum*. Alcoa Laboratories, 1987.

(2) See for example: (a) Serna, C. J.; White, J. L.; Hem, S. L. *Soil. Sci.* 1977, 41, 1009. (b) Hsu, P. H.; Bates, T. F. *Mineral Mag.* 1964, 33, 749. (c) Willstätter, R.; Kraut, H.; Erbacher, O. *Chem. Ber.* 1925, 588, 2448.

(3) Green, R. H.; Hem, S. L. *J. Pharm. Sci.* 1974, 63, 635.

(4) Adkins, A. *J. Am. Chem. Soc.* 1922, 44, 2175.

(5) Teichner, S. J.; Nicolaon, G. A.; Vicarini, M. A.; Gardes, G. E. *E. Adv. Colloid Interface Sci.* 1976, 5, 245 and references therein.

(6) Yoldas, B. E. *J. Mater. Sci.* 1975, 10, 1856.

(7) (a) Yoldas, B. E. *J. Mater. Sci.* 1977, 12, 1203. (b) Yoldas, B. E. *Am. Ceram. Bull.* 1980, 59, 479.

(8) Alumoxanes, $[\text{Al}(\text{O})(\text{X})]_n$, have traditionally been defined as oligomeric or polymeric materials consisting of an Al-O backbone with pendant substituents X.

(9) Andrianov, K. A.; Zhadanov, A. A. *J. Polym. Sci.* 1958, 30, 513.

(10) (a) Colclough, R. O. *J. Polym. Sci.* 1959, 34, 178. (b) Colclough, R. O. *J. Polym. Sci.* 1960, 48, 273.

(11) Vandenberg, E. J. *J. Polym. Sci.* 1960, 47, 486.

(12) Longiave, C.; Castelli, R. *J. Polym. Sci.* 1963, C4, 387.

* To whom all correspondence should be addressed.

Interest in alkylaluminumoxanes was renewed during the 1980s, by the work of Kaminsky, in the application of methylaluminumoxane (MAO), $[\text{Al}(\text{O})\text{Me}]_n$, as a component of highly active catalysts for the polymerization of ethylene and propylene.¹⁴

Despite all the applications of alumoxanes, no structural picture has emerged that comes close to explaining, and more importantly, predicting the chemistry of alumoxanes. This would seem amiss in view of their undoubted industrial importance. Thus, alumoxanes are best described as "black box" materials, with their preparation and chemistry on the fringe between science and art. In an effort to redress this problem, we have undertaken a detailed spectroscopic investigation into the structure of triethylsilyloxy-substituted alumoxanes. The results of this work and the isolation of a related decaaluminum cluster are presented herein.

Results and Discussion

1. Synthesis and Characterization of $[\text{Al}(\text{OSiEt}_3)_3]_2$. In 1958 Andrianov reported⁹ that the interaction of Et_3SiOH with Al metal, at 150 °C, led to the formation of $[\text{Al}(\text{OSiEt}_3)_3]_2$ (eq 5). In our hands, however,



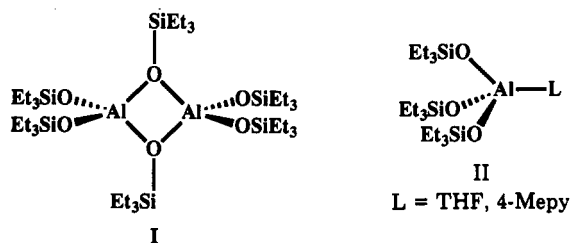
these reaction conditions led to a product contaminated with significant quantities of $\text{O}(\text{SiEt}_3)_2$. The formation of $\text{O}(\text{SiEt}_3)_2$ is undoubtedly due to the dehydration of the silanol at this elevated temperature (eq 6). Attempts to



purify the aluminum siloxide resulted only in further decomposition. We have, therefore, developed an alternative low-temperature route to $[\text{Al}(\text{OSiEt}_3)_3]_2$, which involves the reaction of AlMe_3 with Et_3SiOH , in Et_2O , at -10 °C, and results in the quantitative formation of $[\text{Al}(\text{OSiEt}_3)_3]_2$ (eq 7).



As is common for siloxide and alkoxide complexes of aluminum,¹⁵ $[\text{Al}(\text{OSiEt}_3)_3]_2$ exists as a dimer, I, in both solution and the gas phase, as determined by osmometry and mass spectroscopy, respectively (see Experimental Section).



The ^1H , ^{13}C , ^{17}O , and ^{29}Si NMR spectra of $[\text{Al}(\text{OSiEt}_3)_3]_2$ are consistent with the presence of both bridging and terminal siloxy groups, in a ratio of 1:2 (see Experimental Section and Table I). The unequivocal assignment of the terminal siloxy resonances was made by comparison with the respective spectra for $\text{Al}(\text{OSiEt}_3)_3(\text{THF})$ and $\text{Al}(\text{OSiEt}_3)_3(4\text{-Mepy})$ in which only terminal siloxy groups

Table I. Heteroatom NMR Chemical Shifts^a

compound	^{29}Si	^{17}O	^{27}Al
$[\text{Al}(\text{OSiEt}_3)_3]_2$	25.2 5.2	30.3 (1220) 15.8 (830)	57.1 (4400)
$\text{Al}(\text{OSiEt}_3)_3(\text{THF})$	2.3	b	56.2 (4200)
$\text{Al}(\text{OSiEt}_3)_3(4\text{-Mepy})$	2.5	15.2 (325)	56.2 (3800)
alumoxane 1	6.9	c	c
alumoxane 2	6.9	c	c
alumoxane 3	7.2	c	6.2 (1300) ^d
alumoxane 4	25.5 5.5	71.0 (366) 34.3 (524) 15.6 (463)	51.6 (10160) 4.1 (6) ^e
$[\text{Al}_4(\text{OH})(\text{OSiEt}_3)_{11}]_n$ (5)	25.2 6.9	31.7 (680) 15.2 (633)	649 (6100) 9.2 (700)
$\text{Al}_{10}(\text{OH})_{16}(\text{OSiEt}_3)_{14}$ (6)	7.7 6.8 5.4	53.6 (226) 31.3 (580) 15.3 (645)	75.3 (4700) 8.9 (310)

^a $W_{1/2}$ values in hertz are given in parentheses. ^b ^{17}O signal for complex masked by that of THF. ^c Insufficient solubility to obtain solution spectra. ^d Solid-state ^{27}Al CPMAS. ^e Minor constituent.

are present (II). The ^{27}Al spectra of $[\text{Al}(\text{OSiEt}_3)_3]_2$, $\text{Al}(\text{OSiEt}_3)_3(\text{THF})$, and $\text{Al}(\text{OSiEt}_3)_3(4\text{-Mepy})$ (Table I) are consistent with four-coordinate aluminum centers.¹⁶

2. Synthesis and Characterization of (Triethylsilyloxy)alumoxanes. It has been previously reported that alumoxanes may be obtained utilizing the following routes: (a) heating the precursor compound under a stream of moist air,⁹ (b) addition of water to a solution of the precursor compound,^{7,17} and (c) reaction of methylalumoxane with protic reagents.¹⁸ We have used each of these methods to synthesize triethylsilyloxy-substituted alumoxanes so as to compare and contrast the physical, and spectroscopic properties of the materials thus produced.

Samples of $[\text{Al}(\text{OSiEt}_3)_3]_2$ were heated under a stream of moist air, at temperatures sufficient to remove, by distillation, the Et_3SiOH produced (bp 75 °C, 24 mmHg). Temperatures of 130 °C, for alumoxane 1, and 170 °C, for alumoxane 2, were employed to investigate the effect of temperature on the chemical composition of the alumoxane. The alumoxanes produced by this method are white amorphous powders, which have negligible solubility in nonpolar organic solvents but are moderately soluble in DMSO.

The thermogravimetric analysis of $[\text{Al}(\text{OSiEt}_3)_3]_2$, heated under a stream of wet air at the analogous conditions required for the formation of 1 and 2, takes ca. 6–7 h for mass loss to cease and the alumoxane to reach constant composition. Since the rate of hydrolysis appears to be dependent on not only the temperature but also the particle size of the precursor, it is difficult to prepare consistent batches of either 1 or 2. It is due to the difficulty in monitoring the hydrolysis reaction at high temperatures that we investigated the "sol-gel" formation of alumoxanes.

A THF solution of $[\text{Al}(\text{OSiEt}_3)_3]_2$ was exposed to the atmosphere to allow slow hydrolysis by the diffusion of ambient moisture. The solution becomes increasingly viscous as hydrolysis proceeds until a colorless gel is formed. No further hydrolysis is observed beyond this point. The gel produced may be separated, washed with THF, and dried under vacuum to give a transparent colorless glass, alumoxane 3. The glass exhibits similar solubility to the powders described above. To gain further

(13) Sakharovskaya, G. B. *Zh. Obshch. Khim.* 1969, 39, 788.

(14) (a) Sinn, H.; Kaminsky, W.; Vollmer, H. J.; Woldt, R. *Angew. Chem.* 1980, 92, 396. (b) Sinn, H.; Kaminsky, W. *Adv. Organomet. Chem.* 1980, 18, 99. (c) Kaminsky, W. *Makromol. Chem., Rapid Commun.* 1983, 4, 417. (d) Kaminsky, W.; Luker, H. *Makromol. Chem., Rapid Commun.* 1984, 5, 225.

(15) Bradley, D. C. *Adv. Chem. Ser.* 1959, 23, 10.

(16) See: (a) Benn, R.; Rufinska, A.; Lehmkühl, H.; Janssen, E.; Kruger, C. *Angew. Chem., Int. Ed. Engl.* 1983, 22, 779. (b) Apblett, A. W.; Barron, A. R. *Organometallics* 1990, 9, 2137.

(17) Pasynkiewicz, S. *Polyhedron* 1990, 9, 429 and references therein.

(18) (a) Kimura, Y.; Sugaya, S.; Ichimura, T.; Taniguchi, *Macromolecules* 1987, 20, 2329. (b) Kimura, Y.; Furukawa, M.; Yamane, H.; Kitao, T. *Macromolecules* 1989, 22, 79. (c) Kimura, Y.; Tanimoto, S.; Yamane, H.; Kitao, *Polyhedron* 1990, 9, 371.

Table II. High-Resolution XPS Peak Positions and Relative Elemental Composition for Alumoxanes 1-4

alumoxane	peak position ^a			elemental ratio ^b	
	O _{1s}	Si _{2p}	Al _{2p}	O:Al	Si:Al
1	531.6	101.6	74.3	2.0	0.19 (±0.03)
2	531.6	101.5	74.3	2.1	0.15 (±0.02)
3	531.3	100.5	74.2	2.0	0.18 (±0.02)
4	531.6	100.7	74.7	2.1	0.98 (±0.03)

^a Peak positions in electronvolts; charge referenced to graphitic carbon C_{1s} = 284.4 eV. ^b Average based on the analysis of multiple samples, range given in parentheses.

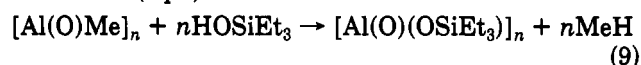
understanding of the formation of alumoxane 3 by the sol-gel route, we have investigated the reaction of [Al(OSiEt₃)₃]₂ with aliquots of H₂O.

To a weighed quantity of [Al(OSiEt₃)₃]₂ in THF was added an accurately determined amount of water, 0.125-3 equiv/aluminum. Gelation to form 3 occurred in all cases with more than 1.25 equiv of H₂O/aluminum. In the remaining cases the resulting soluble aluminum species were isolated and characterized by NMR spectroscopy (see below).

The insolubility of the alumoxanes 1-3, presumably due to either their high molecular weights or high hydroxide content (see below), prompted us to investigate the synthesis of hydrocarbon soluble alumoxanes. Kimura and co-workers¹⁸ have reported the synthesis of the hydrocarbon soluble isopropoxy-substituted alumoxane from the reaction of isopropyl alcohol with methylalumoxane (eq 8). Similarly, the addition of Et₃SiOH to [Al(O)Me]_n



results in the formation of a triethylsiloxy-substituted alumoxane (eq 9).



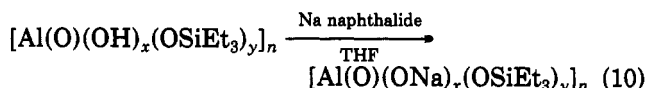
The isolated alumoxane exists as a waxy white solid, which is highly soluble in nonpolar organic solvents. The average molecular weight of the condensate was determined by osmometry to be ca. 1300 g/mol, which corresponds to a minimum of seven degrees of polymerization. It is therefore perhaps better to think of the alumoxane 4 as being an aluminum cluster, which may be a fragment of the alumoxanes 1-3. It should be noted, however, that unlike the materials produced by the hydrolysis routes, alumoxane 4 is not hydrolytically stable.

The elemental composition of alumoxanes 1-4 may be determined by X-ray photoelectron spectroscopy (XPS). The high resolution Al_{2p}, Si_{2p}, and O_{1s} peak positions are given in Table II; all high-resolution spectra were charge referenced to the adventitious carbon present in the XPS samples (see Experimental Section). The relative elemental composition was obtained from the integration of the peaks, calibrated and corrected by suitable response factors, and correlated with standard samples. The calibrated O:Al and Si:Al ratios determined in this manner are given in Table II. The O:Al ratio, ca 2, is essentially constant between all the samples. This is consistent with the general formulation, previously proposed for alumoxanes, i.e., [Al(O)(X)]_n, X = R, OR, OSiR₃, etc.^{9,17,18} However, the Si:Al ratio in the hydrolytically stable alumoxanes, 1-3 is significantly lower than that indicated by this formulation. The low silicon content may be accounted for by the presence of hydroxide groups as indicated by IR and NMR spectroscopies.

The IR spectra of alumoxanes 1-3 show broad absorption bands centered between 3372 and 3397 cm⁻¹ typical of hydrogen-bonded hydroxy groups. In addition, the IR

spectrum of alumoxane 1 contains a sharp absorption band at 3858 cm⁻¹ due to non-hydrogen-bonded hydroxy moieties. Proton-deuterium exchange of the hydroxy groups of 1-3 may be effected by stirring a suspension of the alumoxanes in D₂O. It is clear from mass balance and elemental composition that no further condensation of the alumoxane occurs. The ²H spectra of deuterated 2 and 3 each show a single resonance (δ 0.39 and 0.38, respectively) which may be assigned to the hydrogen-bonded hydroxy groups present in the polymer.¹⁹ Alumoxane 1 displays a similar resonance (δ 0.40) as well as a lower intensity signal at 0.82 ppm due to non-hydrogen-bonded hydroxides. The results for the deuterium exchange and ²H NMR spectroscopy are therefore consistent with the corresponding IR spectra of the alumoxanes.

The hydroxide content of alumoxanes 1-3 may be determined quantitatively by their metalation with sodium naphthalide (eq 10), followed by the determination of the



Na:Al ratio by XPS. The O:Al and Si:Al ratios are unchanged on metalation, indicating that reaction occurs specifically at the hydroxide groups. Furthermore, the sum of the Si:Al and Na:Al ratios is close to unity, i.e., $x + y \approx 1$, indicating a general formula of [Al(O)(OH)_x(OSiEt₃)_{1-x}]_n for the hydrolytically stable alumoxanes 1-3. The extent of hydrolysis of the alumoxane, as measured by the magnitude of x , varies over a surprisingly narrow range (0.81 < x < 0.85) despite the hydrolysis occurring in both solution and the solid state, as well as over a considerable temperature range.

The IR spectrum of alumoxane 4 indicates the absence of hydroxide groups, a fact confirmed by the XPS measurements (Table II), which show a Si:Al ratio of 0.98 (±0.03) consistent with the formulation [Al(O)(OSiEt₃)_n].

The ¹H and ¹³C NMR spectra of 1-3 are essentially identical and indicate the presence of a single siloxy environment in each. The chemical shifts are upfield with respect to those observed for both the bridging and terminal siloxides in [Al(OSiEt₃)₃]₂. This would suggest that the alumoxane siloxides are in a different chemical environment from those of the precursor. Although the methyl and methylene peaks are well resolved in the solution ¹³C NMR spectra, only a single broad resonance (δ 6.85) is observed in the ¹³C CPDAS spectrum of 2. Despite this, the solid-state NMR does indicate that the solution NMR spectra are representative of the bulk material. The presence of a single siloxy environment in alumoxanes 1-3 is also demonstrated by ²⁹Si NMR spectroscopy. A single resonance is observed at a position distinct from those of the precursor [Al(OSiEt₃)₃]₂ but is within the range observed for terminal siloxides (see below). In addition, the presence of a single siloxide environment indicates that no hydrolysis has occurred at the silicon.

The ¹H NMR spectra of the alumoxanes produced from the reaction of [Al(OSiEt₃)₃]₂ with x equiv of H₂O/aluminum demonstrated the presence of two main types of triethylsiloxy environments, which by comparison with the ¹H NMR spectrum of [Al(OSiEt₃)₃]₂ can be assigned as bridging [δ 1.03 (CH₃), 0.92 (CH₂)] and terminal [δ 1.2-1.1 (CH₃), 0.8-0.7 (CH₂)]. While only one type of bridging siloxide is observed, the terminal siloxide multiplet consists of several overlapping signals. These were

(19) Although the proton-deuterium exchange was not undertaken for 1 it would undoubtedly be the same as observed for 3, given the similarity of their IR spectra.

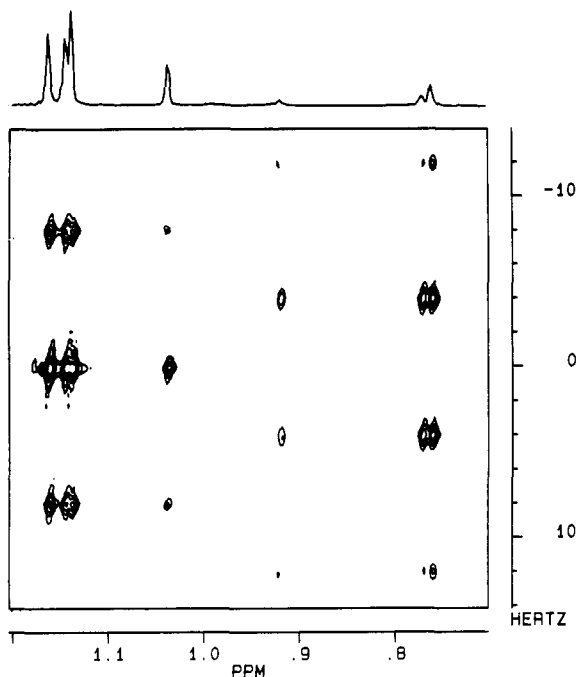


Figure 1. J -resolved ^1H NMR spectrum of the alumoxane isolated from the reaction of $[\text{Al}(\text{OSiEt}_3)_3]_2$ with 1.0 equiv of H_2O /aluminum.

subsequently resolved utilizing a standard homonuclear J -resolved two-dimensional NMR experiment²⁰ (see Figure 1). Two methylene environments (δ 0.77 and 0.73) and three methyl environments (δ 1.16, 1.14, and 1.11) were thus identified. This disparity between the number of methyl environments versus methylene ones may be possibly attributed to hindered rotation about the Si-O bond of one of the triethylsiloxy substituents, since the resonances at 1.14 and 1.11 ppm coalesce above 60 °C. No other significant change in the ^1H NMR spectra was observed as a function of temperature, for any of the species. Increasing the extent of hydrolysis leads to a corresponding increase in the relative intensities of the signals at 1.16 and 0.73 ppm so that just prior to gellation (i.e., 1.125 equiv of H_2O) they are the strongly predominant ^1H NMR signals.

The initial ^{13}C NMR assignments were based on normal ^1H -decoupled ^{13}C spectra plus CH_2 and CH_3 subspectra obtained using DEPT spectral editing.²¹ To unambiguously complete the assignment, heteronuclear (^1H - ^{13}C) correlated two-dimensional experiments were performed.²² Figure 2 demonstrates the result obtained for the alumoxane derived from the addition of 1 equiv of H_2O . The resonances for the carbons of the bridging triethylsiloxy and thus determined to be 7.10 (CH_3) and 6.81 (CH_2) ppm. The hindered rotation of one of the nonbridging triethylsiloxy substituents leads to the observation and three methyl resonances (δ 7.78, 7.71, and 7.63) while there are only two corresponding methylene signals (δ 7.80 and 7.73). As with the ^1H NMR spectra, heating to 60 °C causes the methyl resonances at 7.78 and 7.63 ppm to coalesce, confirming their assignment to the nonrotating siloxide environment. The ^{13}C NMR resonances favored by increased hydrolysis are those for the methylene carbon at 7.80 ppm and the methyl carbon at 7.33 ppm.

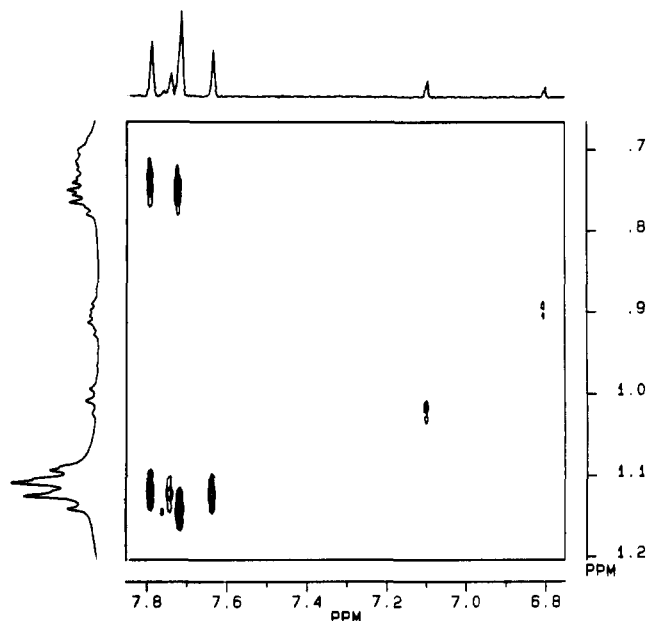


Figure 2. ^1H - ^{13}C correlation NMR spectrum of the alumoxane isolated from the reaction of $[\text{Al}(\text{OSiEt}_3)_3]_2$ with 1.0 equiv of H_2O /aluminum.

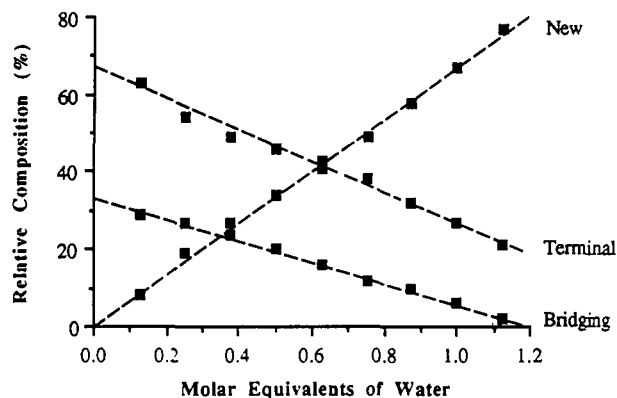


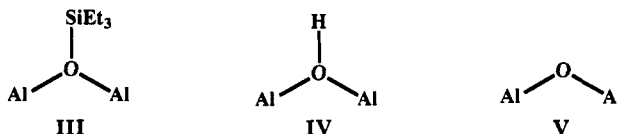
Figure 3. Plot of percentage of each siloxide environment present in the isolated alumoxanes as a function of the number of equiv of H_2O added/aluminum.

Unfortunately, due to the overlapping nature of the peaks in the ^1H and ^{13}C NMR spectra for $x = 0.125$ – 1.125 , we are unable to readily determine, by peak integration, the relative amount of each siloxide environment. On the other hand, ^{29}Si NMR provides a convenient probe to follow the changes in the siloxide environment during hydrolysis. A plot of the percentage siloxides present for each of the three observed environments in the isolated materials versus the extent of hydrolysis, x , is shown in Figure 3. The two environments, δ 25.5 and 5.3, which decrease with increasing x may be assigned to bridging and terminal siloxides, respectively, due to their similarity to those found for $[\text{Al}(\text{OSiEt}_3)_3]_2$. The third resonance is almost identical to that observed for the isolated alumoxanes 1–3 (see Table I). From Figure 3, we can conclude that two distinct structural changes are occurring. First, the decrease in the relative amount of bridging siloxide environments (III) with increased hydrolysis is undoubtedly due to steric factors which favor the formation of

(20) Bax, A. *Two Dimensional Nuclear Magnetic Resonance in Liquids*; D. Reidel: Holland, 1982.

(21) Doddrell, D. M.; Pegg, D. T.; Bendall, M. R. *J. Magn. Reson.* 1982, 48, 323.

(22) Bax, A.; Morris, G. A. *J. Magn. Reson.* 1981, 42, 501.



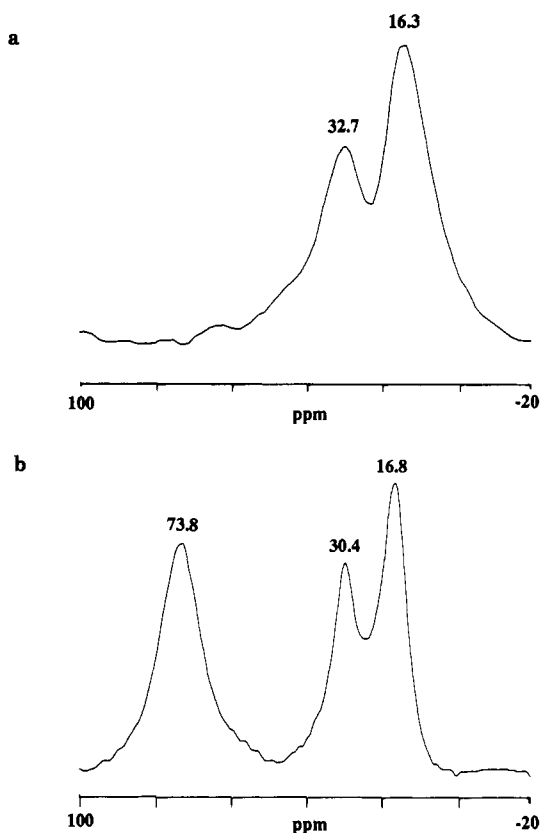
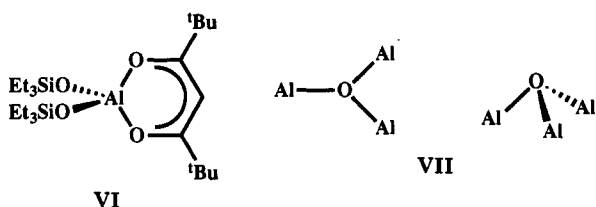


Figure 4. ^{17}O NMR spectrum of isolated material from the reaction of $[\text{Al}(\text{OSiEt}_3)_3]_2$ with 0.25 (a) and 1.0 (b) equiv of H_2O /aluminum.

hydroxy (IV) or oxo bridges (V). Second, the coordination environment of the terminal siloxide ligand is altered with increased hydrolysis. We have previously observed²³ for a series of aluminum alkoxide oligomers that a direct correlation exists between the NMR chemical shift of the terminal aluminum ligands and the Al_xO_x ring size. At a low degree of hydrolysis the predominant environment is similar to that observed for $[\text{Al}(\text{OSiEt}_3)_3]_2$ in which the aluminum is within a four-membered ring (I). While at higher extents of hydrolysis the predominant peak (δ 7.2) is more similar to that observed for $\text{Al}(\text{OSiEt}_3)_2(\text{tmhd})$ (tmhd = 2,2,6,6-tetramethylheptanedionate, VI), δ 8.4,²⁴ in which the aluminum is within a six-membered ring. It therefore follows that the new terminal environment may be assigned to a siloxide coordinated to an aluminum atom within a six-membered ring.



Due to the low solubility of alumoxanes 1-3, we were unable to obtain either ^{17}O or ^{27}Al solution NMR spectra; however, the alumoxanes produced by the stepwise hydrolysis of $[\text{Al}(\text{OSiEt}_3)_3]_2$, $x < 1.25$ per aluminum, were all sufficiently soluble to enable ^{17}O and ^{27}Al NMR to be obtained. At low extents of hydrolysis (<0.75 equiv) the

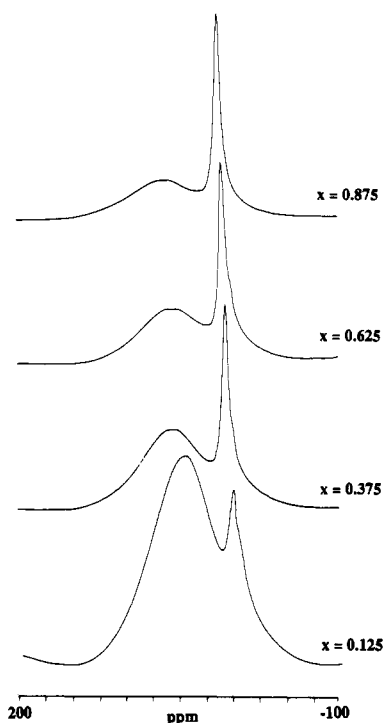


Figure 5. ^{27}Al NMR spectra of isolated alumoxanes from the reaction of $[\text{Al}(\text{OSiEt}_3)_3]_2$ with x equiv of H_2O /aluminum.

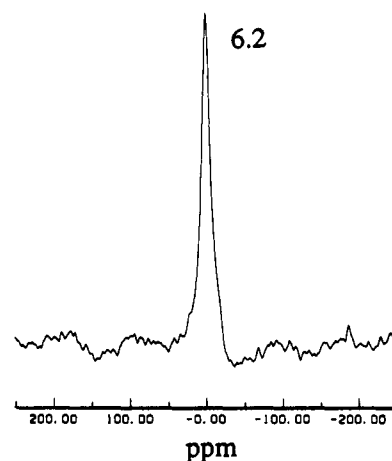


Figure 6. ^{27}Al CPMAS NMR spectrum of alumoxane 3.

^{17}O NMR of the isolated aluminum species (e.g., Figure 4a) shows no oxoaluminum species and is similar to that of $[\text{Al}(\text{OSiEt}_3)_3]_2$. Above 0.75 equiv of H_2O /aluminum an additional peak is observed (73.8 ppm), the relative intensity of which increases with increased hydrolysis (Figure 4b). We conclude that this is due to the aluminum oxo group (V or VII) and *not* a siloxide. This assignment has been confirmed by the use of ^{17}O -enriched (11.5%) water, since the intensity of this peak is greatly enhanced as compared to the high field signals. It should be noted that with insufficient drying of the alumoxanes a signal at 2.5 ppm is present which we have shown to be due to coordinated triethylsilanol.

The variation in the ^{27}Al NMR spectra of the isolated species with increments of added water is shown in Figure 5. Peaks are observed for both four-coordinate (δ 56.2) and six-coordinate (δ 7.8) aluminum. The relative abundance of six-coordinate aluminum increases as hydrolysis becomes more extensive until the hydrolytically stable alumoxane, 3, is formed. At this point the aluminum is primarily in a six-coordinate environment as determined by the solid-state ^{27}Al CPMAS NMR spectrum of 3 (Figure

(23) Apblett, A. W.; Rogers, J.; Barron, A. R. *Abstracts of Papers*; Canadian Chemical Congress: Hamilton, Ontario, Canada, 1991.

(24) Apblett, A. W.; Barron, A. R. *Abstracts of Papers*; 202th National Meeting of the American Chemical Society, New York, NY, 1991; American Chemical Society: Washington, DC, 1991.

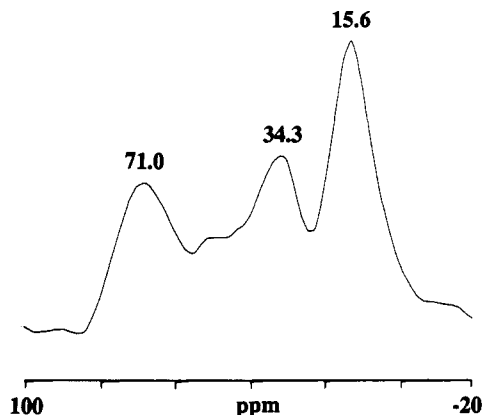


Figure 7. ^{17}O NMR spectrum of alumoxane 4, showing the presence of oxo (71.0 ppm) as well as both bridging (34.3 ppm) and terminal (15.6 ppm) siloxide oxygen environments.

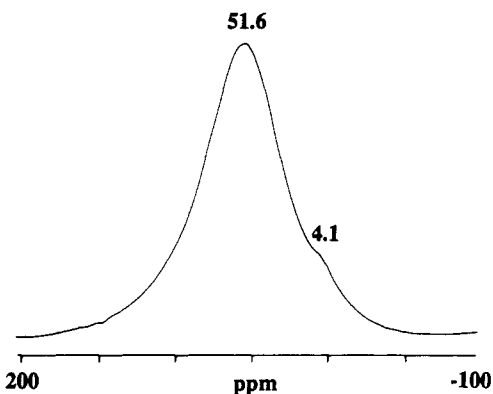


Figure 8. ^{27}Al NMR spectrum of alumoxane 4, showing the presence of both four- and six-coordinate aluminum.

6). We believe it is reasonable to propose, therefore, the the six-coordinate aluminum represents the core of the alumoxane, while the four-coordinate aluminum centers are the edge or end groups (supporting evidence for this is given below).

The ^1H , ^{13}C , and ^{29}Si NMR spectra of alumoxane 4 demonstrates the presence of two siloxide environments in a ratio of ca. 1:3. By comparison to $[\text{Al}(\text{OSiEt}_3)_2]$ these may be tentatively assigned as bridging and terminal, with the latter predominating. The solution ^{17}O and ^{27}Al NMR spectra of 4 (Table I) are readily observed in a mixture of pentane and C_6D_6 (1:1). The ^{17}O NMR spectrum of 4 shows three broad peaks (Figure 7). We assign the downfield signal (δ 71.0) to an aluminum-oxo species, either $\text{Al}_3(\mu_3\text{-O})$ or $\text{Al}_2(\mu_2\text{-O})$, while the upfield signals may be assigned to bridging (δ 34.3) and terminal (δ 15.6) siloxide environments. The solution ^{27}Al NMR spectrum of 4 (Figure 8) indicates the presence of primarily four-coordinate, as well as a trace of six-coordinate aluminum.

As has been mentioned above, we have used XPS spectral peak areas for the determination of the elemental composition in the alumoxanes; however, XPS peak positions may also be used to determine the gross chemical environment of specific elements.²⁵ Figure 9 shows the high-resolution $\text{Al}(2p)$ spectra for alumoxane 3 and several aluminum-containing minerals. It is readily apparent that the electronic environment around aluminum in 1-3 (see Table II and Figure 10) is similar to that in the mineral boehmite, whose formula, $[\text{Al}(\text{O})(\text{OH})]_n$, is obviously related to that of the alumoxanes 1-3, i.e., $[\text{Al}(\text{O})(\text{OH})_x(\text{OSiEt}_3)_{3-x}]_n$.

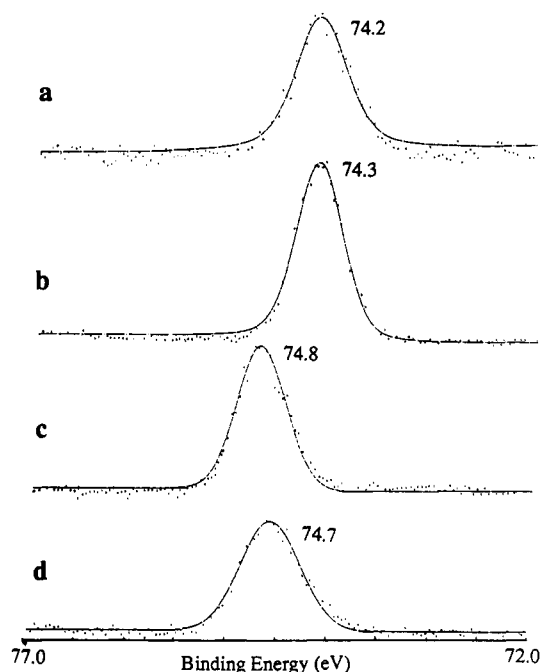


Figure 9. High-resolution $\text{Al}(2p)$ curve fitted XPS spectral components for alumoxane 1 (a), boehmite (b), alumina (c), and aluminum silicate (d).

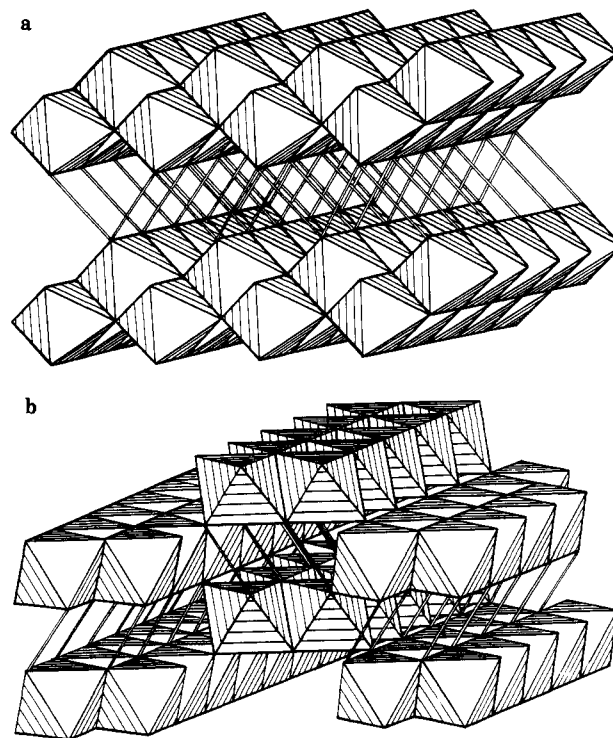


Figure 10. Structures of (a) boehmite and (b) diaspore. Oxygen atoms are to be imagined at the vertices of each octahedron which has an aluminum atom at its center. The double lines indicate hydrogen bonds.

3. Proposed Structure for Siloxyalumoxanes. On the basis of the known structure of dialkylsiloxane polymers, VIII, alumoxanes were originally proposed to have a linear chain structure consisting of alternate aluminum and oxygen atoms, IX.^{9,17,18} Such a structure would require the aluminum to have a coordination number of three, which is rare and exists only in the gas phase²⁶ or in com-

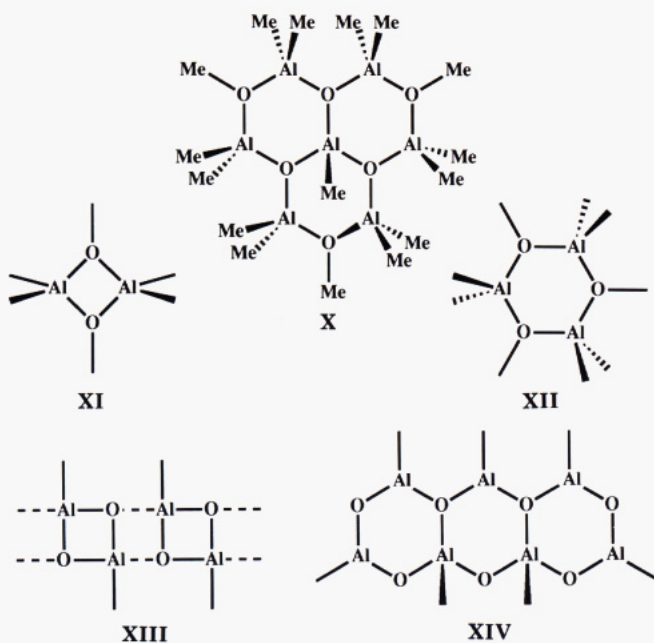
(25) Barr, T. L. *Appl. Surf. Sci.* 1983, 15, 1.

(26) Almenningsen, A.; Halvorsen, S.; Haaland, A. *Acta. Chem. Scand.* 1971, 25, 1937.



pounds in which oligomerization is hindered by sterically bulky ligands.²⁷ Since it is common for aluminum to maximize its coordination number, through the formation of dimers and trimers¹⁵ via bridging ligands, the majority of workers have proposed that the aluminum has a coordination number of four or higher.

The structural similarity of the $[\text{Al}_7(\text{O})_3(\text{OMe})_3(\text{Me})_{12}]^-$ anion²⁸ (X) to the structures of dimeric (XI) and trimeric (XII) alkoxide compounds of aluminum prompted many groups to propose structures based on open four- and six-membered rings (e.g. XIII and XIV).^{17,29,30}



The vast majority of reports in the literature have assumed that all alumoxanes have the general formula $[\text{Al}(\text{O})(\text{X})]_n$, where $\text{X} = \text{R}, \text{OR}, \text{OSiR}_2, \text{O}_2\text{CR}$, etc. Where hydroxide groups have been detected, their content has been proposed to be low and constant.³⁰ We have shown, however, that hydrolytically stable siloxaluminum oxanes are best described by the general formula $[\text{Al}(\text{O})(\text{OH})_x(\text{OSiR}_3)_{1-x}]_n$, the extent of hydroxide formation (the magnitude of x) is significant, being dependent on the method and temperature of alumoxane synthesis (see above) as well as the identity of the alkyl substituents.³¹

(27) (a) Sheldrick, G. M.; Sheldrick, W. S. *J. Chem. Soc. A* **1969**, 2279. (b) Starowieyski, K. B.; Pasynkiewicz, S.; Skowronska-Ptasinska, M. *J. Organomet. Chem.* **1975**, *90*, C43. (c) Jerius, J. J.; Hahn, J. M.; Rahman, A. F. M. M.; Mols, O.; Ilsley, W. H.; Oliver, J. P. *Organometallics* **1986**, *5*, 1812. (d) Uhl, W. *Z. Naturforsch.* **1988**, *43b*, 1113. (e) Shreve, A. P.; Mulhaupt, R.; Fultz, W.; Calabrese, J.; Robbins, W.; Ittel, S. D. *Organometallics* **1988**, *7*, 2543. (f) Healy, M. D.; Wierda, D. A.; Barron, A. R. *Organometallics* **1988**, *7*, 2543.

(28) Atwood, J. L.; Hrnec, D. C.; Priester, R. D.; Rogers, R. D. *Organometallics* **1983**, *2*, 985.

(29) See for example: (a) Storr, A.; Jones, K.; Laubengayer, A. W. *J. Am. Chem. Soc.* **1968**, *90*, 3173. (b) Boleslawski, M.; Pasynkiewicz, S.; Kunicki, A.; Serwatowski, J. *J. Organomet. Chem.* **1976**, *116*, 285. (c) Siergiejczyk, L.; Boleslawski, M.; Synoradzki, L. *Polimery (Warsaw)* **1986**, 397.

(30) Bradley, D. C.; Lorimar, J. W.; Prevedorov-Demas, C. *Can. J. Chem.* **1971**, *49*, 2310.

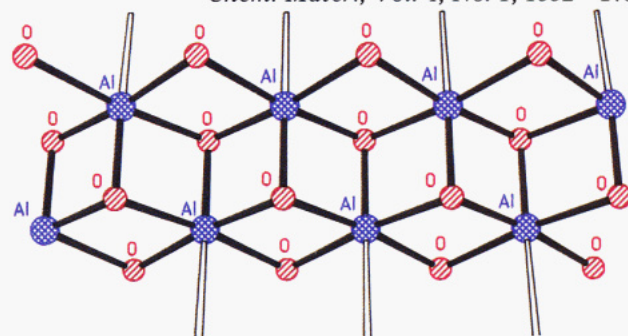


Figure 11. Core structure of $[\text{Al}(\text{O})(\text{OH})]_n$.³²

The upper limit of hydroxide formation in an alumoxane, i.e., $x = 1$, would result in a formulation the same as found for the mineral boehmite and its polymorph diasporite, $[\text{Al}(\text{O})(\text{OH})]_n$, the structures of which are shown in Figure 10.³² It is only logical to expect that if the transition between an alumoxane and boehmite or diasporite is continuous then the core structure would be the same in each. A fragment of the common core of the minerals is shown in Figure 11. The structure may be considered as consisting of two parallel but staggered chains of six-coordinate aluminum atoms, linked by oxygens μ_3 -capping alternate faces and μ_2 -bridging the sides of the chain. The remaining coordination site on the aluminum centers are occupied by the μ_2 -bridging oxygen atom of the neighboring chains. The arrangement of these interchain bridges is the factor which differentiates boehmite and diasporite (Figure 10).

Since we have shown by ²⁷Al NMR spectroscopy that stable alumoxanes contain primarily six-coordinate aluminum and that the electronic environment around these aluminum centers as determined by XPS is close to that in boehmite, we propose that the aluminum-oxygen core structure in siloxaluminum oxanes is the same as that present in boehmite and diasporite. Although *direct* crystallographic evidence to support this proposal is at present unavailable (see below), it is clearly entirely feasible based on literature precedents for a wide range of main-group and transition-metal clusters.

The smallest discernible fragment of the boehmite core, the M_3O_4 unit (XV, cf. Figure 11), has previously been observed in aluminum³³ as well as tin³⁴ and molybdenum³⁵ clusters. M_4O_6 fragments (XVI, cf. Figure 11), on the other



hand, have been crystallographically characterized for cobalt³⁶ and molybdenum.³⁴ However, the best supporting

(31) (a) Apblett, A. W.; Barron, A. R. *The Second International Ceramic Science and Technology Congress*; Orlando, FL, 1990, Abstract 65-SIP-90C. (b) Apblett, A. W.; Barron, A. R. *Ceramic Transactions, Advanced Composite Materials: Processing Microstructures, Bulk and Interfacial Properties, Characterization Methods, and Applications*; Sacks, M. D., Ed.; The American Ceramic Society, Inc.: Westerville, OH, 1991, Vol. 19, p 35.

(32) (a) Milligan, W. D.; McAtee, J. L. *J. Phys. Chem.* **1956**, *60*, 273. (b) Hoppe, W. *Z. Kristallogr.* **1942**, *104*, M-17. (c) Busing, W. R.; Levy, H. A. *Acta Crystallogr.* **1958**, *11*, 798.

(33) Yanovskii, A. I.; Turova, N. Ya.; Kozlova, N. I.; Struchkov, Yu. T. *Koord. Khim.* **1987**, *13*, 242.

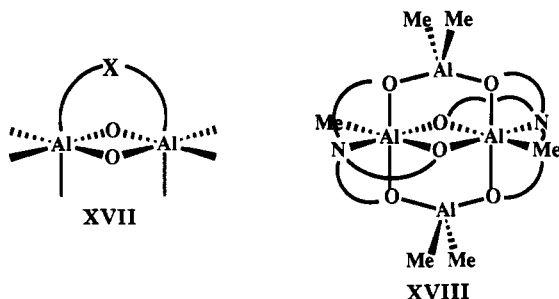
(34) See for example: (a) Holmes, R. R.; Kumara-Swamy, K. C.; Schmid, C. G.; Day, R. O. *J. Am. Chem. Soc.* **1988**, *110*, 7060. (b) Day, R. O.; Holmes, J. M.; Chandrasekhar, V.; Holmes, R. R. *J. Am. Chem. Soc.* **1987**, *109*, 940. (c) Holmes, R. R. *Acc. Chem. Res.* **1989**, *22*, 190.

(35) Liu, S.; MA, L.; McGavty, D.; Zubieta, J. *Polyhedron* **1990**, *9*, 1541.

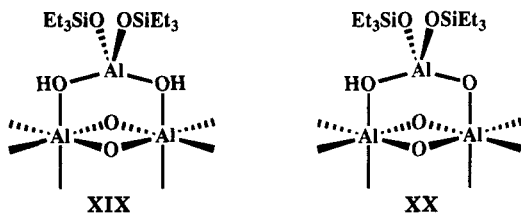
evidence for our proposal are the recently reported clusters $\{\text{Ni}_8\text{O}_{14}[(\text{OSiPh})_6]_2\}^{37}$ and $\text{Ca}_9(\text{OCH}_2\text{CH}_2\text{OMe})_{18}(\text{HOCH}_2\text{CH}_2\text{OMe})_2$,³⁸ both of which have boehmite type metal-oxygen cores surrounded by a supporting organic framework.

It should be obvious, however, that whereas the minerals have infinite structures, alumoxanes must have a finite size. Thus there must be either end or edge groups encapsulating the boehmite-like core. We have shown above, and previously,³¹ that low molecular weight alumoxanes, i.e., where hydrolysis is incomplete, contain significant four-coordinate aluminum centers; it is likely, therefore, that these four-coordinate aluminum atoms comprise the end groups. To explain the presence of a four-coordinate aluminum periphery to the boehmite core, one must logically assume that there are chemical groups unrelated to the core structure. In addition, since the core is composed of fused Al_2O_2 four-membered rings, the edge groups must be able to bridge between two adjacent aluminum atoms (XVII).

We have previously reported the synthesis and structural characterization of $\{[\text{N}(\text{CH}_2\text{CH}_2\text{O})_3]\text{Al}_2\text{Me}_3\}_2$ (XVIII).³⁹ In



this molecule the two six-coordinate octahedral aluminum atoms are bridged by a 'Me₂AlO₂' unit, whose oxygen atoms are associated with the two triethoxy-amine ligands. In the case of the siloxy-alumoxanes 1-3 these oxygens would be hydroxy or oxo ligands and the terminal groups would be OSiEt₃ ligands. Thus, we propose that the edges and ends of the alumoxane core are occupied by either $[(\text{Et}_3\text{SiO})_2\text{Al}(\text{OH})_2]^-$ (XIX) or $[(\text{Et}_3\text{SiO})_2\text{Al}(\text{OH})\text{O}]^{2-}$ (XX)



moieties. This picture is also consistent with the observed ²⁹Si NMR spectra, which indicate the siloxides to be coordinated to a four-coordinate aluminum within a six-membered cycle.

On the basis of NMR spectral data, the structure of alumoxane 4 is clearly related more closely to that of $[\text{Al}(\text{OSiEt}_3)_3]_2$ than that of alumoxane 1-3. Although we have as of this time insufficient data to propose a definite structural model we have shown that alumoxane 4 consists of predominantly four or, given the large line width in the ²⁷Al NMR spectrum, possibly five-coordinate aluminum centers. The siloxides are in both bridging and terminal

(36) Buchanan, R. M.; Fitzgerald, B. J.; Pierpont, C. G. *Inorg. Chem.* 1979, 18, 3439.

(37) Levitsky, M. M.; Schegolikina, O. I.; Zhadanov, A. A.; Igonin, V. A.; Ouchinnikov, Yu. E.; Shklover, V. E.; Struchkov, Yu. T. *J. Organomet. Chem.* 1991, 401, 199.

(38) Goel, S. C.; Matchett, M. A.; Chiang, M. Y.; Buhro, W. E. *J. Am. Chem. Soc.* 1991, 113, 1844.

(39) Healy, M. D.; Barron, A. R. *J. Am. Chem. Soc.* 1989, 111, 398.

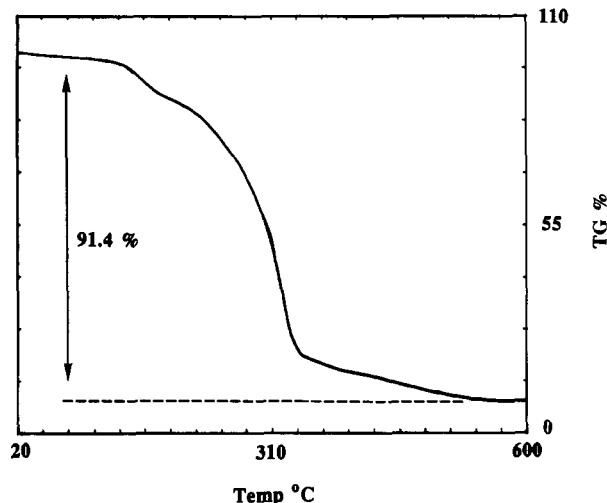


Figure 12. Thermogravimetric analysis of $[\text{Al}_4(\text{OH})(\text{OSiEt}_3)_{11}]_n$ (6).

environments. In addition, from the ²⁹Si NMR peak positions we can infer that the structure consists of four- rather than six-membered aluminum-oxygen rings. Studies are under way to further elucidate the structure of this class of alumoxane and their relationship to MAO.

4. Synthesis and Structural Characterization of $\text{Al}_{10}(\text{OH})_{16}(\text{OSiEt}_3)_{14}$. As we have noted above, we have been unable to obtain direct X-ray crystallographic conformation of our proposed structure for the hydrolytically stable alumoxanes 1-3. However, while characterizing the alumoxanes formed from the reaction of $[\text{Al}(\text{OSiEt}_3)_3]_2$ with low molar equivalent aliquots of H₂O (0.25-0.75), we observe that their thermolysis resulted in the formation of $[\text{Al}(\text{OSiEt}_3)_3]_2$ as the only volatile product and a new involatile, hydrocarbon soluble "alumoxane".

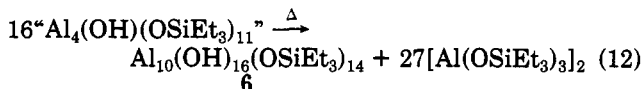
The reaction of $[\text{Al}(\text{OSiEt}_3)_3]_2$ with 0.25 mol equiv of water per aluminum in THF produces, after removal of the solvent and the byproduct Et₃SiOH (30 °C, 10⁻⁴ Torr), a waxy white solid. Under these drying conditions, a constant weight of product is eventually reached that corresponds to the formation of $[\text{Al}_4(\text{OH})(\text{OSiEt}_3)_{11}]_x$ (5, eq 11). Alumoxane 5 has been characterized by IR, NMR,

$$2[\text{Al}(\text{OSiEt}_3)_3]_2 + \text{H}_2\text{O} \rightarrow$$

$$[\text{Al}_4(\text{OH})(\text{OSiEt}_3)_{11}]_x + \text{Et}_3\text{SiOH} \quad (11)$$

and X-ray photoelectron spectroscopies; see Experimental and Table I.

Heating alumoxane 5 in vacuo (50 °C) results in significant weight loss and the irreversible formation of $\text{Al}_{10}(\text{OH})_{16}(\text{OSiEt}_3)_{14}$ (6) as the only involatile product. Mass spectroscopy of 5 (50 °C) demonstrates that the volatiles are composed exclusively of $[\text{Al}(\text{OSiEt}_3)_3]_2$ (eq 12).



The thermogravimetric analysis (TGA) of 6 is shown in Figure 12. It can be seen that although under atmospheric pressure the rate of conversion of 5 to 6 is limited by the low volatility of the $[\text{Al}(\text{OSiEt}_3)_3]_2$ side-product (sublimation temperature = 225 °C, 760 mmHg), the final mass is entirely consistent with eq 12.

It is important to note that the possibility that 5 was a mixture of 6 plus unreacted $[\text{Al}(\text{OSiEt}_3)_3]_2$ may be eliminated since separate signals attributable to $[\text{Al}(\text{OSiEt}_3)_3]_2$ are observed in the ²⁹Si NMR spectrum, when the latter compound was added to a solution of 6. The spectroscopic

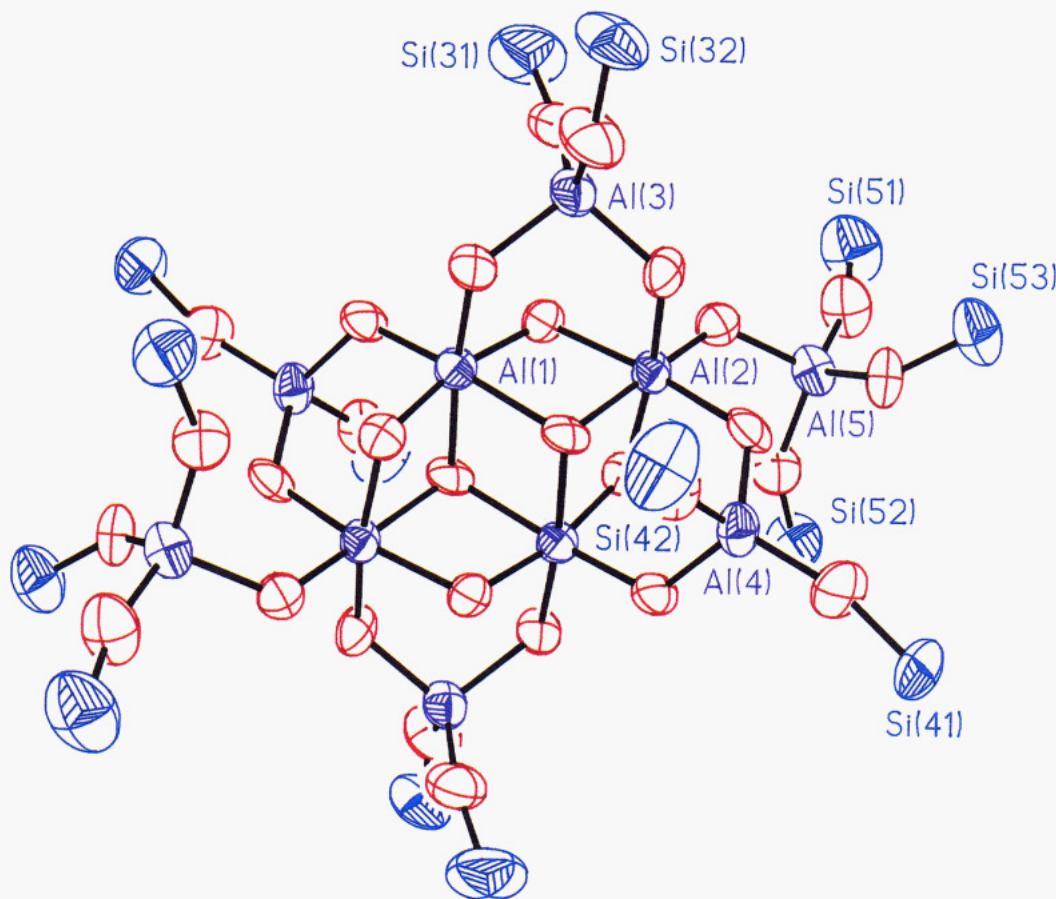


Figure 13. Molecular structure of $\text{Al}_{10}(\text{OH})_{16}(\text{OSiEt}_3)_{14}$ (**6**). Thermal ellipsoids are drawn at the 50% level, and all carbon and hydrogen atoms have been omitted for clarity.

Table III. Selected Bond Lengths (Å) in $\text{Al}_{10}(\text{OH})_{16}(\text{OSiEt}_3)_{14}$ (6**)**

Al(1)–O(12)	1.834 (9)	Al(1)–O(121)	1.97 (1)
Al(1)–O(21A)	1.814 (8)	Al(1)–O(13)	1.87 (1)
Al(1)–O(12A)	1.94 (1)	Al(1)–O(14A)	1.86 (1)
Al(2)–O(121)	1.970 (9)	Al(2)–O(12)	1.87 (1)
Al(2)–O(21)	1.90 (1)	Al(2)–O(23)	1.89 (1)
Al(2)–O(24)	1.89 (1)	Al(2)–O(25)	1.81 (1)
Al(3)–O(23)	1.80 (1)	Al(3)–O(13)	1.834 (8)
Al(3)–O(32)	1.70 (1)	Al(3)–O(31)	1.68 (1)
Al(4)–O(24)	1.798 (9)	Al(4)–O(14)	1.81 (1)
Al(4)–O(42)	1.71 (1)	Al(4)–O(41)	1.68 (1)
Al(5)–O(51)	1.70 (1)	Al(5)–O(25)	1.82 (1)
Al(5)–O(53)	1.74 (1)	Al(5)–O(52)	1.73 (1)
Si(32)–O(32)	1.62 (1)	Si(31)–O(31)	1.55 (1)
Si(42)–O(42)	1.64 (1)	Si(41)–O(41)	1.60 (1)
Si(52)–O(52)	1.62 (1)	Si(51)–O(51)	1.58 (1)
O(121)–Al(1A)	1.94 (1)	Si(53)–O(53)	1.63 (1)
O(14)–Al(1A)	1.86 (1)	O(21)–Al(1A)	1.814 (8)

characterization of **5** and **6** (vide infra) also precludes this theory.

Compound **6** is soluble in nonpolar hydrocarbon solvents, and crystals suitable for X-ray diffraction studies were obtained by cooling ($-20\text{ }^\circ\text{C}$) a saturated pentane solution. Full characterization of **6** has been enabled by IR, NMR, and X-ray photoelectron spectroscopies (see below, Table I, and Experimental Section).

The molecular structure of **6** has been determined by X-ray diffraction. Selected bond lengths and angles are given in Tables III and IV, respectively. The structure consists of a neutral centrosymmetric decaaluminum cluster, the core of which is shown with atom labels in Figure 13. The labeling scheme for the oxygen, silicon, and carbon atoms is based on their coordination to the aluminum atoms. Thus oxygen atoms bridging or capping only aluminum atoms are numbered with respect to the aluminum atoms; for example, O(121) is bonded to Al(1), Al(2), and Al(1A), while O(12) is bonded to Al(1) and Al(2).

Table IV. Selected Bond Angles (deg) in $\text{Al}_{10}(\text{OH})_{16}(\text{OSiEt}_3)_{14}$ (6**)**

O(121)–Al(1)–O(12)	77.4 (4)	O(121)–Al(1)–O(12A)	77.8 (5)
O(121)–Al(1)–O(13)	94.6 (5)	O(12)–Al(1)–O(13)	87.1 (5)
O(12)–Al(1)–O(12A)	93.3 (5)	O(13)–Al(1)–O(12A)	172.2 (5)
O(121)–Al(1)–O(21A)	91.4 (4)	O(12)–Al(1)–O(21A)	168.2 (6)
O(13)–Al(1)–O(21A)	97.7 (5)	O(12)–Al(1)–O(14A)	95.0 (4)
O(12A)–Al(1)–O(21A)	80.5 (5)	O(21A)–Al(1)–O(14A)	95.0 (4)
O(121)–Al(1)–O(14A)	165.1 (6)	O(12)–Al(2)–O(21)	91.5 (5)
O(12A)–Al(1)–O(14A)	90.0 (5)	O(13)–Al(1)–O(13A)	97.7 (5)
O(121)–Al(2)–O(12)	76.7 (4)	O(121)–Al(2)–O(23)	91.7 (5)
O(121)–Al(2)–O(21)	77.9 (4)	O(12)–Al(2)–O(23)	169.5 (5)
O(12)–Al(2)–O(24)	165.1 (5)	O(121)–Al(2)–O(24)	89.7 (4)
O(23)–Al(2)–O(24)	89.1 (5)	O(12)–Al(2)–O(23)	85.2 (5)
O(121)–Al(2)–O(25)	171.5 (6)	O(21)–Al(2)–O(24)	91.7 (5)
O(21)–Al(2)–O(25)	94.7 (5)	O(12)–Al(2)–O(25)	99.6 (5)
O(24)–Al(2)–O(25)	94.7 (5)	O(23)–Al(2)–O(25)	95.7 (5)
O(13)–Al(3)–O(23)	102.5 (5)	O(13)–Al(3)–O(31)	112.0 (5)
O(23)–Al(3)–O(31)	112.3 (7)	O(13)–Al(3)–O(32)	103.8 (6)
O(23)–Al(3)–O(32)	107.0 (6)	O(31)–Al(3)–O(32)	117.9 (6)
O(14)–Al(4)–O(24)	101.1 (5)	O(14)–Al(4)–O(41)	111.1 (6)
O(24)–Al(4)–O(41)	114.0 (5)	O(14)–Al(4)–O(42)	102.7 (5)
O(24)–Al(4)–O(42)	103.9 (6)	O(41)–Al(4)–O(42)	121.5 (7)
O(25)–Al(5)–O(51)	109.9 (6)	O(25)–Al(5)–O(52)	101.3 (5)
O(51)–Al(5)–O(52)	116.9 (7)	O(25)–Al(5)–O(53)	100.7 (6)
O(51)–Al(5)–O(53)	115.1 (5)	O(52)–Al(5)–O(53)	110.7 (5)
Al(1)–O(121)–Al(2)	98.4 (4)	Al(1)–O(121)–Al(1A)	102.2 (5)
Al(2)–O(121)–Al(1A)	96.8 (6)	Al(1)–O(12)–Al(2)	107.3 (5)
Al(2)–O(21)–Al(1A)	104.1 (6)	Al(1)–O(13)–Al(3)	121.0 (7)
Al(2)–O(23)–Al(3)	123.2 (6)	Al(4)–O(14)–Al(1A)	123.4 (6)
Al(2)–O(24)–Al(4)	123.8 (5)	Al(2)–O(25)–Al(5)	126.9 (6)
Al(3)–O(31)–Si(31)	165 (1)	Al(3)–O(32)–Si(32)	152.6 (7)
Al(4)–O(41)–Si(41)	164.5 (6)	Al(4)–O(42)–Si(42)	150.3 (8)
Al(5)–O(51)–Si(51)	165.3 (8)	Al(5)–O(52)–Si(52)	142.1 (7)
Al(5)–O(53)–Si(53)	140.3 (5)		

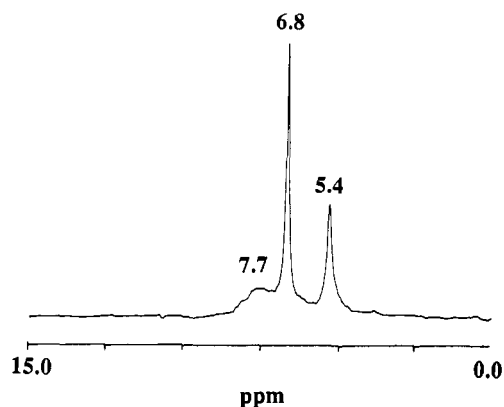
N.B. O(21) is bonded to Al(2) and Al(1A). The designation of the triethylsiloxy groups is based on the aluminum atoms to which they are coordinated; for example, Al(3) has two triethylsiloxy groups consisting of O(31), Si(31), C(311)–C(316) and O(32), Si(32), C(321)–C(326).

Compound **6** consists of four chemically distinct aluminum environments (two six-coordinate and two four-coordinate), five hydroxide environments, and two triethyl

Table V. ^1H , ^{13}C , and ^{29}Si NMR Spectral Assignments for the Triethylsiloxy Groups in $\text{Al}_{10}(\text{OH})_{16}(\text{OSiEt}_3)_{14}$ (6)

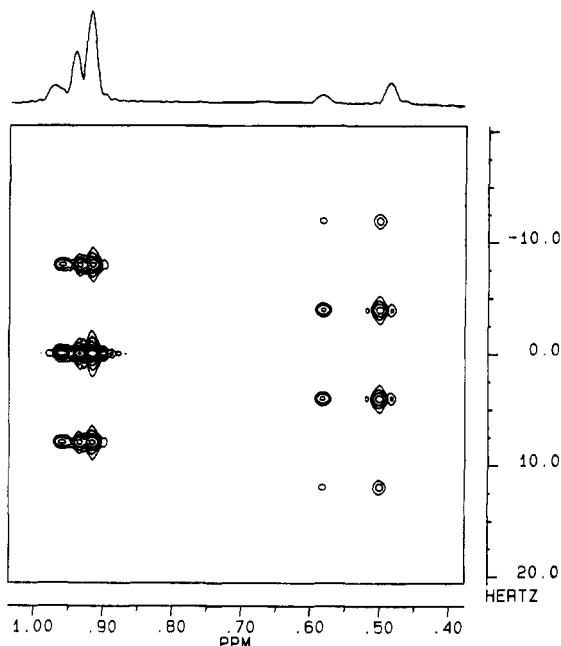
silicon ^a	$^1\text{H}^b$		$^{13}\text{C}^b$		$^{29}\text{Si}^b$
	CH_2	CH_3	CH_2	CH_3	
31, 32	0.49	0.93	7.20	7.31	6.8
41	0.49	0.93	6.67	7.18	7.7
42	0.58	0.96	5.80	6.56	
51, 52, 53	0.50	0.92	7.13	7.25	5.4

^aFor atom labeling see Figure 14. ^bSpectra obtained in CDCl_3 , chemical shift (δ) in ppm relative to SiMe_4 (external).

**Figure 14.** ^{29}Si NMR spectrum of $\text{Al}_{10}(\text{OH})_{16}(\text{OSiEt}_3)_{14}$.

siloxide environments. The Al_4O_6 core of 6 contains four six-coordinate aluminum atoms [Al(1), Al(1A), Al(2), and Al(2A)] joined by two μ_3 - and four μ_2 -hydroxide groups and is best considered to consist of two face-shared aluminum-oxygen cubes in which two of the diagonally opposing aluminum vertices are absent (cf. Figure 13). Each of the remaining four external faces of the cubes are bridged via the two μ_2 -hydroxide groups of four $[(\text{HO})_2\text{Al}(\text{OSiEt}_3)_2]$ moieties [i.e., Al(3), Al(3A), Al(4), and Al(4A)]. This bridging unit results in the formation of a fused six- and four-membered Al_3O_4 ring system (XIX) similar to those found in the structures of $\{\text{Al}_2\text{Me}_3[(\text{OCH}_2\text{CH}_2)_3\text{N}]\}_2$ (XVIII)³⁹ and the $[\text{Al}_3(\text{H}_3\text{Cit})_3(\text{OH})-(\text{H}_2\text{O})]^{4-}$ anion (H_3Cit = citric acid).⁴⁰ The sixth-coordination sites of the aluminum atoms positioned on the external vertices of the core, Al(2) and Al(2A), are occupied by hydroxides which bridge to $\text{Al}(\text{OSiEt}_3)_3$ groups Al(5) and Al(5A), respectively. Although bridging and capping hydroxides are common in aluminum chemistry, these are rare examples of structurally characterized unsupported hydroxide bridges.

Despite the relatively high esd's (see Experimental Section) the Al-O bond distances are in three distinct ranges; μ_3 capping hydroxides [1.95 (1)–1.97 (1) Å], μ_2 bridging hydroxides [1.79 (1)–1.90 (1) Å], and terminal siloxides [1.67 (1)–1.73 (1) Å]. The μ_2 -OH groups bridging a six- and the four-coordinate aluminum atoms in the $[(\text{HO})_2\text{Al}(\text{OSiEt}_3)_2]$ moieties are positioned asymmetrically with the shorter bond distance to the latter. This asymmetry is expected from a consideration of the relative *s* and *p* contributions in the respective Al-O bonds, i.e., six coordinate (*p*) > four coordinate (*sp*³).⁴¹ However, the μ_2 -OH bridge between Al(2) and Al(5) is symmetric, the reason for this anomaly is unclear. The six-coordinate aluminum atoms exhibit elongated trigonal distortion [*trans*-O-Al-O = 165.2 (6)–172.2 (5)°]. The four-coordi-

**Figure 15.** *J*-resolved ^1H NMR spectrum of $\text{Al}_{10}(\text{OH})_{16}(\text{OSiEt}_3)_{14}$.

nate aluminum centers each have distorted tetrahedral geometries with the largest interligand angles being those between the terminal siloxide oxygens. The Al-O-Si bond angles [140.3 (5)–165.3 (8)°] are all within the range associated with terminal siloxides and alkoxides,⁴² while all the Si-O bonds are within the ranges observed previously, 1.612–1.666 Å.⁴³

The ^1H , ^{13}C , and ^{29}Si chemical shift assignments of the triethylsiloxy groups in 6 are given in Table V. As indicated, the ^{29}Si NMR spectrum contains three resonances; a sharp singlet at 6.8 ppm and two broader resonances at 7.7 and 5.4 ppm (see Figure 14). Integration yields a ratio for silicon atoms in each environment of 4:4:6, respectively. On this basis, then, the signal at 5.4 ppm may be ascribed to the six silicon atoms associated with the two terminal $\text{Al}(\text{OSiEt}_3)_3$ groups [Si(51), Si(52), and Si(53)]. This assignment is supported by the fact that the shift falls within the normal range observed for such a moiety. If it is assumed that the broadening of this signal and the one at 7.7 ppm is due to restricted movement of the $[(\text{HO})_2\text{Al}(\text{OSiEt}_3)_2]$ unit as a result of steric interaction between triethyl siloxide groups on Al(4) and Al(5), it follows that the latter resonance is due to Si(41) and Si(42). The peak at 6.8 ppm is attributed to Si(31) and Si(32), since according to the solid-state structure they are nearly equivalent.

The Et_3SiO groups of 6 give rise to ^1H NMR resonances that consist of several overlapping triplets between 0.90 and 1.0 ppm, overlapping quartets between 0.43 and 0.53 ppm, and a single well-resolved quartet centered at 0.58 ppm. The latter peak had an integrated intensity of 12 versus 74 for the remaining quartets. Resolution of the multiplets was accomplished by use of *J*-resolved two-dimensional NMR spectroscopy²⁰ (see Figure 15). Thus, three methyl (δ 0.96, 0.93, and 0.92) and three methylene (δ 0.58, 0.50, and 0.49) environments were identified. The connectivity between the methyl and methylene functionalities was established via ^1H - ^1H COSY 2D NMR spectroscopy⁴⁴ (see Figure 16) while ^1H - ^{29}Si connectivity was determined by obtaining selectively decoupled ^{29}Si

(40) Feng, T. L.; Gurian, P. L.; Healy, M. D.; Barron, A. R. *Inorg. Chem.* 1990, 29, 408.

(41) Albright, T. A.; Burdett, J. K.; Whangbo, M. H. *Orbital Interactions in Chemistry*; Wiley: New York, 1985; Chapter 14.

(42) See for example: Oliver, J. P.; Kumar, R. *Polyhedron* 1990, 9, 409.

(43) Healy, M. D.; Barron, A. R. *J. Organomet. Chem.* 1990, 381, 165 and references therein.

(44) (a) Ave, W. P.; Bartholdi, E.; Ernst, R. R. *J. Chem. Phys.* 1976, 64, 2229. (b) Nagayama, K.; Kumar, A.; Wuthrich, K.; Ernst, R. R. *J. Magn. Reson.* 1980, 40, 321.

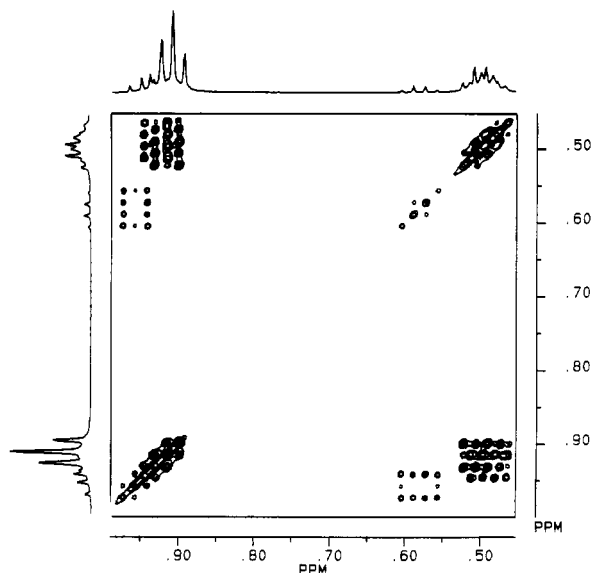


Figure 16. ^1H - ^1H correlation NMR spectrum of $\text{Al}_{10}(\text{OH})_{16}(\text{OSiEt}_3)_{14}$.

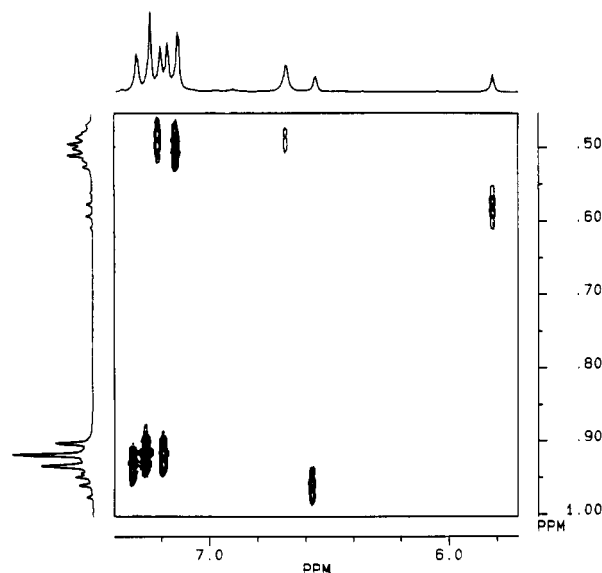


Figure 17. ^1H - ^{13}C correlation NMR spectrum of $\text{Al}_{10}(\text{OH})_{16}(\text{OSiEt}_3)_{14}$.

NMR spectra in which each methylenic ^1H resonance was irradiated. The results are listed in Table V. Finally, the original assignment of the ^{29}Si NMR resonance at 7.7 ppm was confirmed by the observation of NOE enhancement of the ^1H NMR signals due to the methyl groups associated with Si(41) and Si(42) when those of the terminal Al(OSiEt_3) $_3$ were irradiated. From the solid-state structure it is clear that the triethylsiloxy groups on Al(5) are in closer proximity to those on Al(4) [Si(41)---Si(52) = 6.62 Å, Si(41)---Si(53) = 5.60 Å, Si(42)---Si(53) = 6.90 Å] than those on Al(3) [Si(31)---Si(51) = 7.82 Å, Si(32)---Si(53) = 7.11 Å] reinforcing this assignment.

The ^{13}C NMR spectrum of 6 was obtained utilizing conditions which allowed for NOE suppression and complete relaxation of nuclei. Thus, eight signals were obtained at 7.31, 7.25, 7.20, 7.18, 7.13, 6.67, 6.56, and 5.80 ppm, with the integrated intensities of 12:18:12:6:18:6:6:6, respectively. The ^{13}C NMR signals for the ethyl groups attached to Si(41) and Si(42) are completely resolved into two equal intensity sets. The assignment of all the ^{13}C NMR signals was accomplished using ^1H - ^{13}C correlated 2D NMR²² (see Figure 17).

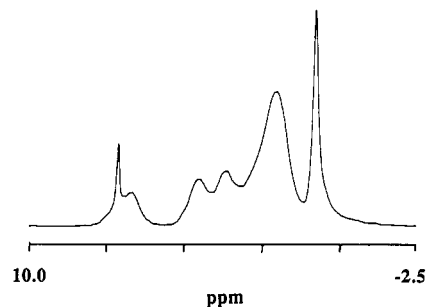


Figure 18. ^2H NMR spectrum of $\text{Al}_{10}(\text{OH})_{16}(\text{OSiEt}_3)_{14}$.

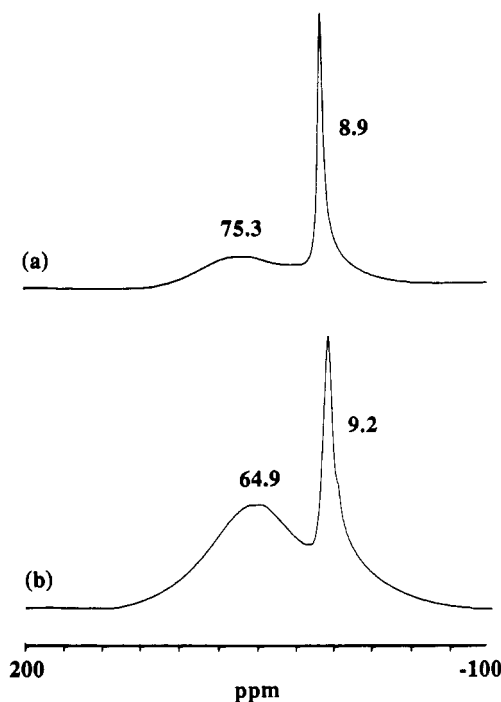


Figure 19. ^{27}Al NMR spectrum of $\text{Al}_{10}(\text{OH})_{16}(\text{OSiEt}_3)_{14}$ (a) and the alumoxane $[\text{Al}_4(\text{OH})(\text{OSiEt}_3)_{11}]_x$ isolated from the reaction of $[\text{Al}(\text{OSiEt}_3)_3]_2$ with 0.25 equiv of H_2O /aluminum (b).

The signals due to the hydroxyl groups of 6 are difficult to discern as a result of their broad nature and overlap with the siloxide resonances. To overcome this problem, 6 was prepared using D_2O and the ^2H NMR spectrum was obtained (Figure 18). On the basis of integrated intensity (8 deuteriums) the signal at 2.1 ppm can be unequivocally assigned to those deuterium atoms attached to O(13), O(23), O(14), and O(24) and their symmetry equivalents; i.e., the hydroxyls which bridge the core six-coordinate aluminum atoms and the external four-coordinate Al(OSiEt_3) $_2$ centers. The two equal intensity (2 deuteriums) signals at 4.6 and 3.7 ppm may be tentatively assigned to the two different types of deuterium attached to the three-coordinate oxygen atoms that bridge six-coordinate aluminum centers [O(12), O(21), and their symmetry equivalents]. Unfortunately, these two environments cannot be readily distinguished. The deuterium atoms attached to the four-coordinate oxygen atoms [O(121) and O(121A)] would be expected to be acidic, and, as such, the lowest field resonance at 6.8 ppm may be attributed to them. Finally, the signal at 0.84 ppm may be assigned to the hydroxyls which connect the Al(OSiEt_3) $_3$ units to the central core [O(25) and O(25A)]. In keeping with the greater flexibility of movement of these hydroxyls and the corresponding decrease in τ_c , this resonance is relatively sharp ($\Delta W_{1/2} = 11.5$ Hz) compared to the other signals ($\Delta W_{1/2} = 30$ Hz).

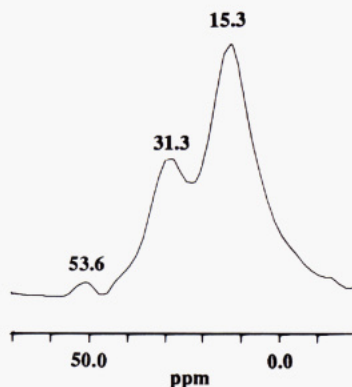


Figure 20. ^{17}O NMR spectrum of $\text{Al}_{10}(\text{OH})_{16}(\text{OSiEt}_3)_{14}$, showing the presence of μ_3 -OH (53.6 ppm), μ_2 -OH (31.3 ppm), and terminal siloxide (15.3 ppm) oxygen environments.

By comparison with **6**, the deuterated analogue of alumoxane **5** has two resonances in its ^2H NMR spectrum at 3.1 and 1.3 ppm in the ratio of 1:2, respectively. The lack of any low-field signals suggests that all the hydroxides in **5** are μ_2 -bridging, and they must undergo considerable structural modification in the formation of **6** from **5**.

The ^{27}Al NMR spectrum of **6** (Figure 19) indicates the presence of both four- and six-coordinate aluminum centers (see Table I); however, it is not possible to resolve the five chemically distinct aluminum environments present in the solid state, i.e., the two six-coordinate, Al(1) and Al(2), and three four-coordinate, Al(3), Al(4), and Al(5). This cannot be attributed to any facile exchange processes since the ^1H , ^{13}C , and ^{29}Si NMR spectra, discussed above, demonstrate the presence of a rigid atomic framework.

The ^{17}O NMR spectrum of **6** shows three broad peaks (Figure 20) at 53.6, 31.3, and 15.3 ppm. The shifts of the latter two compare favorably to the shifts observed for the bridging (δ 30.3) and terminal (δ 15.8) siloxides in $[\text{Al}(\text{OSiEt}_3)_3]_2$ (see Table I). Thus, although the peak at 15 ppm in the ^{17}O NMR spectrum of **6** can be assigned as terminal siloxides, that at 31.3 ppm cannot be due to bridging siloxides since none are present in the structure. We propose, therefore, that this is due to the μ_2 -bridging hydroxides present in the structure of **6**. Finally, the peak at 53.6 ppm in the spectrum of **6** is assigned to the μ_3 -capping hydroxides.

We have previously assigned a resonance (70–75 ppm) in the ^{17}O NMR spectrum of isolated alumoxanes to be due to an aluminum–oxo group and not a siloxide or hydroxide.³¹ The absence of this resonance in the ^{17}O NMR of **6** continues to support this hypothesis.

5. Structural Relationship of $\text{Al}_{10}(\text{OH})_{16}(\text{OSiEt}_3)_{14}$ to Siloxy-Substituted Alumoxanes and the Minerals Boehmite and Diaspore. As outlined above we have proposed that siloxy-substituted alumoxanes consist of an aluminum–oxygen core similar in structure to that found in boehmite and diaspore, surrounded by terminal siloxide groups coordinated to four-coordinate aluminum centers. Although compound **6** contains no oxo groups, and it is clearly not an alumoxane per se, it does contain the salient features of our proposed structure.

A correlation cannot easily be drawn between structural environment and the ^1H and ^{13}C NMR chemical shifts of triethylsiloxy-substituted aluminum compounds. On the other hand, ^{29}Si NMR provides a convenient probe to directly compare siloxide environments. Of the three siloxide environments observed for compound **6** (Table V) only those analogous to Si(31) and Si(32), are found in the isolated alumoxanes. This, therefore, confirms our previous proposal that the terminal siloxide ligands present in the hydrolytically stable siloxy-substituted alumoxanes,

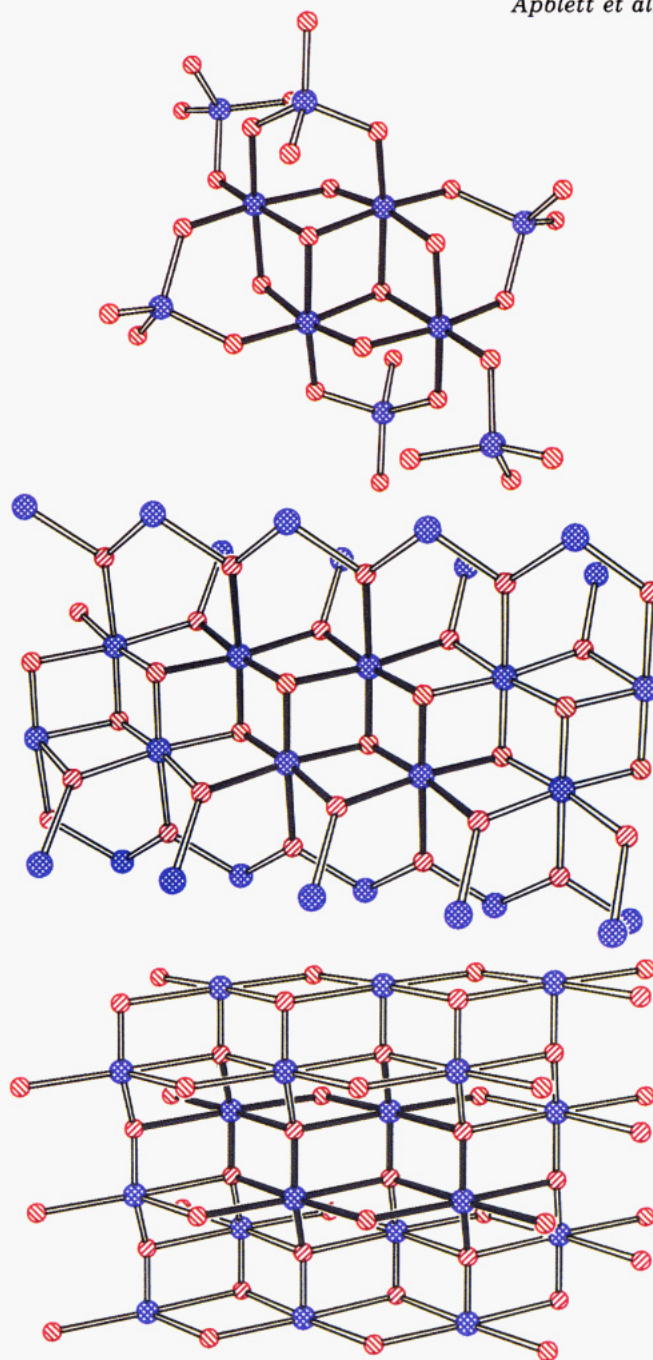


Figure 21. Aluminum–oxygen core structure of $\text{Al}_{10}(\text{OH})_{16}(\text{OSiEt}_3)_{14}$ (a, top). The solid bonds represent the structural fragment present in the minerals diaspore (b, middle) and boehmite (c, bottom). Aluminum atoms shown in purple, hydroxide (shaded top left to bottom right) and oxide (shaded bottom left to top right) oxygen atoms in red.

$[\text{Al}(\text{O})(\text{OH})_{1-x}(\text{OSiEt}_3)_x]_n$ ($0.15 < x < 0.13$), i.e., 1–3, are terminal, bound to four-coordinate aluminum centers within a six-membered Al_3O_3 ring (XIX and XX). Furthermore, it should be noted that resonances similar to that assigned to Si(51)–(53) are observed when the hydrolysis of $[\text{Al}(\text{OSiEt}_3)_3]_2$ is incomplete. It is conceivable, therefore, that a moiety similar to $\text{Al}(5)(\text{OSiEt}_3)_3$ is involved in the hydrolysis–condensation growth of alumoxane macromolecules.

Thus on the basis of an NMR spectroscopic analysis of compound **6** and the alumoxanes derived from the partial hydrolysis of $[\text{Al}(\text{OSiEt}_3)_3]_2$, it is clear that our proposed structural model for the coordination environment for the siloxy substituents on the alumoxanes is indeed valid.

The ^2H NMR spectra of the fully hydrolyzed alumoxanes **2** and **3** indicated the presence of a major hydroxide

environment the chemical shifts for which [(0.40 (2), 0.38 (3) ppm)] are close to two of those observed in 6 (0.37 and 0.46 ppm), and assigned to be a μ_2 -hydroxide (IV) bridging two six-coordinate aluminum centers. The additional minor hydroxide environment observed in 2 (0.82 ppm) is clearly similar to that assigned to be the μ_2 -hydroxide coordinated to the $\text{Al}(\text{OSiEt}_3)_3$ unit. Since this resonance is eliminated when alumoxane 2 is thermally condensed to give 3, it would lend support to the condensation pathway suggested above. The lack of signals due to the $(\text{HO})_2\text{Al}(\text{OSiEt}_3)_2$ unit detected in the ^2H NMR spectra of 2 and 3 is unsurprising since they would only account for ca. 10% of the total, and their large line widths would further hinder detection.

Using ^{27}Al NMR spectroscopic data, we have shown that alumoxanes obtained by the hydrolysis of $[\text{Al}(\text{OSiEt}_3)_3]_2$ contain both four- and six-coordinate aluminum centers, with the relative abundance of the latter increasing as hydrolysis becomes more extensive. We have postulated that the six-coordinate aluminum represents the core of the alumoxane, while the four-coordinate aluminum centers are the edge or end groups. This arrangement is observed in the structure of compound 6, and, since the ^{27}Al NMR spectra of the alumoxane products obtained by the solution hydrolysis of $[\text{Al}(\text{OSiEt}_3)_3]_2$ are similar to that for 6, it is only logical to conclude that the aluminum environments in 6 and the alumoxanes are closely related.

In addition to ^{27}Al NMR spectroscopy, we have used high-resolution Al_{2p} XPS spectral positions to determine that the electronic environment around the core aluminum atoms in triethylsiloxy substituted alumoxanes is close to that in the minerals boehmite and diaspore, $[\text{Al}(\text{O})(\text{OH})]_n$. This result was the initial basis of our proposal for an alumoxane core based on that of boehmite or diaspore. It can be clearly seen from the highlighted sections in Figure 21 that there exists a definite structural similarity between the core of compound 6 (Figure 21a) and the structures of diaspore (Figure 21b) and boehmite (Figure 21c), thus confirming our previous conclusion.

It is interesting to note that the edge-shared octahedral packing of the metal centered polyhedra observed in compound 6, boehmite, and diaspore is not only found in various binary oxides and halides (e.g., CdI_2 and $\alpha\text{-Al}_2\text{O}_3$) but, as mentioned above, also in a wide range of metal oxide, hydroxide, and alkoxide clusters, in particular those of tin,³⁴ molybdenum,³⁵ calcium,³⁸ and nickel,³⁷ suggesting that this core structure is a common motif in inorganic oxygen-donor macromolecules. Given the above we respectfully submit that the structural similarity between minerals and inorganic clusters is a general trend possibly even extending to those present in biological systems, such as the poly-iron core of Ferretin.⁴⁵

Conclusion

We have determined that alumoxanes, prepared by the hydrolysis of $[\text{Al}(\text{OSiEt}_3)_3]_2$, in both the solid state and solution, have the general formula of $[\text{Al}(\text{O})(\text{OH})_x(\text{OSiEt}_3)_{1-x}]_n$. The extent of hydrolysis, as measured by the magnitude of x , varies only slightly with the method and temperature of the alumoxane synthesis. On the basis of spectroscopic evidence and by comparison with the structurally characterized Et_3SiO -substituted aluminum cluster $\text{Al}_{10}(\text{OH})_{16}(\text{OSiEt}_3)_{14}$, literature precedent, and aluminum-containing minerals, we have proposed that siloxy-substituted alumoxanes have a core structure analogous to that found in the minerals boehmite and diaspore, in which the aluminum centers are six-coordinate.

Furthermore, we have proposed that this aluminum oxygen core is encapsulated by terminal Et_3SiO groups bound to four-coordinate aluminum atoms within six-membered rings.

By contrast the alumoxanes formed by the reaction of Et_3SiOH with $[\text{Al}(\text{O})\text{Me}]_n$ have low molecular weight and are essentially hydroxide free. In addition, the siloxides are in environments similar to those present in dimeric $[\text{Al}(\text{OSiEt}_3)_3]_2$.

Experimental Section

General Methods. Microanalyses were performed by Oneida Research Services, Inc., Whitesboro, NY. Mass spectra were obtained by using a JEOL instrument operating at 70 eV. Melting points and thermogravimetric analyses were obtained on a Seiko 200 TG/DTA instrument using a carrier gas of either dry nitrogen or air passed, prior to the furnace, through a glass bubbler containing doubly distilled and deionized water. Molecular weight measurements were made in pentane with the use of an instrument similar to that described by Clark.⁴⁶ IR spectra ($4000\text{--}400\text{ cm}^{-1}$) were recorded on a Nicolet DX-5 FTIR as Nujol or Fluorolube mulls on KBr plates. ^1H and ^{13}C NMR spectra were obtained on a Bruker AM-500 spectrometer, and chemical shifts are reported relative to SiMe_4 in CDCl_3 unless otherwise stated. DEPT²¹ spectra were obtained using the standard pulse program, and a θ pulse of 135° , which yielded CH_2 and CH_3 signals with a 180° phase difference between them. J -resolved 2D ^1H spectra were recorded using a standard pulse sequence,²⁰ a spectral width of 330 Hz, and 1000 and 128 data points in the F2 and F1 domains, respectively. The latter domain was zero-filled to 256W and Lorentzian line-broadening functions equal to the digital resolution were applied to each axis. After transformation, the 2D dataset was tilted to yield a F2 projection corresponding to a broadband-decoupled ^1H experiment. $^1\text{H}\text{--}^{13}\text{C}$ correlated two-dimensional NMR spectra²² were obtained using a standard pulse sequence, sweep widths of ca. 250 and 300 Hz and 1000 and 256 data points for the F2 (^{13}C) and F1 (^1H) domains, respectively. The latter domain was zero-filled to 512 K, and Lorentzian line-broadening functions equal to the digital resolution were applied to each axis prior to transformation. $^1\text{H}\text{--}^1\text{H}$ COSY NMR spectra were collected by use of a standard pulse sequence⁴⁴ with a 45° mixing pulse, a 1–2-s relaxation delay, and a resolution of ca. 4 Hz per point. The FIDs were not weighted before Fourier transformation, and the spectral matrix was symmetrized about the diagonal. ^2H , ^{17}O , ^{27}Al , and ^{29}Si NMR spectra (see text and Tables I and V) were recorded on a Bruker WM-300 spectrometer and chemical shifts are reported versus the residual deuterium in C_6H_6 (7.15 ppm), H_2O , $[\text{Al}(\text{H}_2\text{O})_6]^{3+}$, and Me_4Si (CDCl_3), respectively. Solid-state ^{13}C and ^{27}Al CPMAS NMR were obtained on a Chemagnetics CMC-200A spectrometer operating at spectral frequencies of 50.178 and 51.997 MHz, respectively. Contact times of 10 ms, 4K data points, 60° pulse widths, and relaxation delays of 10 s were utilized in both cases. Chemical shifts are reported relative to the methyl groups in C_6Me_6 (17.3 ppm) and $\text{Al}(\text{N}-\text{O}_3)_3\cdot 6\text{H}_2\text{O}$, respectively. XPS spectra were collected on a Surface Science Instruments Spectrometer (Model SSX-100) with a monochromatized Al-K_α source. Samples of the alumoxanes were prepared by pressing into a disk using a standard IR pellet press. The pressed disks were mounted onto the XPS sample stage with double-sided cellophane tape. The surface of the disk was scraped to remove any contamination incorporated during pressing and finally argon sputtered to constant elemental composition once in the XPS chamber. The spectra were acquired with a 100-eV pass energy and a $600\text{-}\mu\text{m}$ spot size. Radiation damage was insignificant over the acquisition times used. Since the alumoxanes are insulators, they will become electrostatically charged under the X-ray beam. Artifacts of charging include peak shift and peak broadening, thus extensive charge referencing is required. All spectra were charged referenced independently to graphitic carbon ($\text{C}_{1s} = 284.4 \pm 0.1\text{ eV}$)⁴⁷ and gold ($\text{Au}_{4f} = 84.0 \pm 0.1\text{ eV}$).

AlMe_3 as a 2 M solution in hexane (Aldrich) and Et_3SiOH (Huls) were commercial samples and were used without further

(45) For a review see: Lippard, S. J. *Angew. Chem., Int. Ed. Engl.* 1988, 27, 344.

(46) Clark, E. P. *Ind. Eng. Chem., Anal. Ed.* 1941, 13, 820.

(47) Apblett, A. W.; Cheatham, L. K.; Barron, A. R. *J. Mater. Chem.* 1991, 1, 143.

purification. Unless otherwise stated all manipulations were performed under an atmosphere of dry nitrogen. Solvents were dried, distilled, and a degassed before use. Water was doubly distilled and deionized.

The preparation of the alumoxanes 1–4 was carried out on multiple batches (ca. 10 per method). Although some variation was found in the time required for completion of the reaction, the formula of the resulting hydrolytically stable products was found to vary very little between batches (see Table II). The data presented below are therefore for typical runs. N.B. Spectroscopically materials prepared from different batches of a single method were near identical, e.g., integration in the ^1H NMR varied by less than 5%.

[Al(OSiEt₃)₃]₂. A solution of Et₃SiOH (49.65 g, 375.3 mmol) in Et₂O (30 mL) was added dropwise to a Et₂O (50 mL) solution of AlMe₃ (62.6 mL, 2 M in hexane, 125.2 mmol), at -10°C . The reaction was warmed to room temperature and stirred for 12 h. The volatiles were then removed in vacuo to give a waxy white solid: yield 52.6 g, 125.0 mmol; mp 276°C . Anal. Calcd for C₁₈H₄₆AlO₃Si₃: C, 51.0; H, 10.6. Found: C, 51.1; H, 10.8. Molecular weight: calculated for C₃₆H₉₀Al₂O₆Si₆, 841; found 840 (pentane). Mass spectrum: m/z 840 (2M⁺), 811 (2M⁺ - Et). IR (Nujol, cm⁻¹) 1592 (w), 1414 (m), 1260 (w), 1239 (s), 1065 (vs), 1017 (s), 973 (m), 808 (vs), 782 (w), 737 (vs), 689 (vw), 670 (w), 638 (s), 585 (m), 551 (m), 500 (w). NMR (δ , C₆D₆): ^1H 1.14 [6 H, t, $J(\text{H-H}) = 8.0$ Hz, CH₂CH₃ terminal], 1.04 [3 H, t, $J(\text{H-H}) = 7.6$ Hz, CH₂CH₃ bridging], 0.92 [2 H, q, $J(\text{H-H}) = 7.6$ Hz, CH₂ bridging], 0.76 [4 H, q, $J(\text{H-H}) = 8.0$ Hz, CH₂ terminal]; ^{13}C , 7.81 [s, with ^{29}Si satellites $J(\text{Si-C}) = 59.2$ Hz, CH₂ terminal], 7.79 (CH₃ terminal), 7.11 (CH₃ bridging), 6.83 [s, with ^{29}Si satellites $J(\text{Si-C}) = 58.7$ Hz, CH₂ bridging].

Al(OSiEt₃)₃(THF). THF (1 mL) was added to a CDCl₃ solution (2.0 mL) of [Al(OSiEt₃)₃]₂ (2.0 g, 2.36 mmol) in a 10 mm NMR tube. NMR (δ , CDCl₃): ^1H 3.76 [4 H, t, $J(\text{H-H}) = 7.5$ Hz, OCH₂, THF], 1.51 [4 H, t, $J(\text{H-H}) = 7.5$ Hz, OCH₂CH₂, THF], 0.87 [27 H, t, $J(\text{H-H}) = 8.1$ Hz, CH₂CH₃], 0.39 [18 H, q, $J(\text{H-H}) = 8.1$ Hz, CH₂]; ^{13}C 72.5 (OCH₂, THF), 24.3 (OCH₂CH₂, THF), 7.47 (CH₃), 7.30 (CH₂).

Al(OSiEt₃)₃(4-Mepy). 4-Picoline (97 μL , 1.0 mmol) was added to a C₆D₆ solution (2.0 mL) of [Al(OSiEt₃)₃]₂ (0.42 g, 1.0 mmol) in a 10-mm NMR tube. NMR (δ , C₆D₆): ^1H 8.44 [2 H, d, $J(\text{H-H}) = 4.3$ Hz, *o*-CH, 4-Mepy], 6.30 [2 H, d, $J(\text{H-H}) = 4.3$ Hz, *m*-CH, 4-Mepy], 1.54 [3 H, s, CH₃, 4-Mepy], 1.16 [27 H, t, $J(\text{H-H}) = 7.9$ Hz, CH₂CH₃], 0.75 [18 H, q, $J(\text{H-H}) = 7.9$ Hz, CH₂]; ^{13}C , 153.6 (*p*-C, pic), 146.8 (*o*-C, 4-Mepy), 125.8 (*m*-C, 4-Mepy), 20.8 (CH₃, 4-Mepy), 7.81 [CH₂CH₃, and CH₂ with ^{29}Si satellites $J(\text{Si-C}) = 58.6$ Hz].

Synthesis of [Al(OH)_x(OSiEt₃)_{1-x}]_n. Method 1. In a typical run [Al(OSiEt₃)₃]₂ (4.69 g, 5.55 mmol) ground to a fine powder was placed in a preweighed 1-in.-o.d. glass tube. The tube was inserted into a Lindberg tube furnace and connected to a "wet" air supply. The air flow rate was set at 940 mL min⁻¹, and the furnace was heated to 130°C at a rate of 5°C min^{-1} . The flow of water was determined by the mass loss of the H₂O bubbler with time. The precursor gradually changed appearance from waxy/colorless to opaque/white. The precursor was heated at 130°C for 7 h, after which it was cooled to room temperature and washed with benzene (50 mL). The resulting white powder was collected and dried under vacuum: yield 1.17 g. IR (Fluorolube and Nujol, cm⁻¹): 3858 (m, $\nu(\text{OH})$), 3382 (v br m, $\nu(\text{OH})$), 2953 (w), 2924 (vs), 2871 (w), 2854 (m), 1597 (br m), 1460 (s), 1415 (w), 1378 (m), 1246 (m), 1050 (br vs), 1012 (s), 848 (br m), 737 (m), 697 (w). NMR (δ , *d*₆-DMSO): ^1H , 0.88 [3 H, t, $J(\text{H-H}) = 7.9$ Hz, CH₂CH₃], 0.44 [2 H, q, $J(\text{H-H}) = 7.9$ Hz, CH₂]; ^2H (D₂O exchanged, C₆H₆), 0.82 (11%, O-D), 0.40 (89%, O-D...O); ^{13}C , 6.85 (CH₂), 6.18 (CH₂CH₃).

Method 2. Reaction conditions similar to those for method 1 were used except the sample was heated to 170°C for 7 h. IR (Fluorolube and Nujol, cm⁻¹): 3372 (v br m, $\nu(\text{OH})$), 2951 (w), 2920 (vs), 2854 (s), 1593 (br m), 1469 (w), 1419 (vw), 1246 (m), 1049 (vs), 849 (br m), 736 (s), 699 (w). NMR (δ , *d*₆-DMSO): ^1H , 0.88 [3 H, t, $J(\text{H-H}) = 7.9$ Hz, CH₂CH₃], 0.43 [2 H, q, $J(\text{H-H}) = 7.9$ Hz, CH₂]; ^2H (D₂O exchanged, C₆H₆), 0.39 (O-D...O); ^{13}C , 6.84 (CH₂CH₃), 6.17 (CH₂); ^{13}C (CPMAS), 6.85 (CH₂ and CH₂CH₃).

Method 3. A THF solution (50 mL) of [Al(SiOEt₃)₃]₂ (2.0 g, 2.37 mmol) was exposed to the air for 1 week. During this time a colorless jellylike solid was deposited from solution. The reaction

mixture was filtered through a medium-porosity sintered glass filter funnel. The solid was washed with THF (2 \times 25 mL). Drying in vacuo produced a glassy colorless solid: yield 0.45 g. IR (Fluorolube and Nujol, cm⁻¹): 3397 (v br vs, $\nu(\text{OH})$), 2854 (s), 2730 (m), 1505 (br m), 1256 (w), 1236 (w), 1017 (br s), 607 (br vs), 557 (w). NMR (δ , *d*₆-DMSO): ^1H , 0.88 [3 H, t, $J(\text{H-H}) = 7.9$ Hz, CH₂CH₃], 0.44 [2 H, t, $J(\text{H-H}) = 7.9$ Hz, CH₂]; ^2H (D₂O exchanged, C₆H₆), 0.38 (O-D...O); ^{13}C , 6.74 (CH₂), 5.66 (CH₂CH₃).

Method 4. A solution of H₂O (0.49 mL, 27.3 mmol) in THF (10 mL) was added dropwise at 0°C to a solution of AlMe₃ (13.7 mL, 2 M in hexane, 27.4 mmol) over 1 h. (Caution: This is extremely hazardous due to the highly exothermic reaction and the release of methane.) The reaction mixture was warmed to room temperature. After 14 h stirring all the volatiles were removed under vacuum, yielding a white powder (2.0 g). The powder was suspended in pentane (20 mL), and Et₃SiOH (5.5 mL, 35.7 mmol) was added dropwise. After 4 h the volatiles were removed with heating (90°C) in vacuo, to give a colorless solid: yield 5.23 g. Molecular weight: found 1284 (pentane). IR (Fluorolube and Nujol, cm⁻¹): 1260 (w), 1237 (m), 1142 (w), 1066 (vs), 1017 (s), 973 (m), 809 (s), 762 (w), 739 (s), 669 (w), 638 (w), 585 (w), 552 (w), 499 (w). NMR (δ , C₆D₆): ^1H , 1.12 [8 H, t, $J(\text{H-H}) = 8.0$ Hz, CH₂CH₃], 1.03 [3 H, t, $J(\text{H-H}) = 7.9$ Hz, CH₂CH₃], 0.90 [2 H, q, $J(\text{H-H}) = 7.9$ Hz, CH₂], 0.73 [6 H, q, $J(\text{H-H}) = 8.0$ Hz, CH₂]; ^{13}C , 7.72 [s with ^{29}Si satellites $J(\text{Si-C}) = 58.7$ Hz, CH₂], 7.70 (CH₂CH₃), 7.02 (CH₂CH₃), 6.75 [s with ^{29}Si satellites $J(\text{Si-C}) = 52.8$ Hz, CH₂].

Metalation of Alumoxane Polymers. To a stirred suspension of the polymers (ca. 0.5 g) in THF (2 mL) was added dropwise a THF solution of Na naphthalide (1.0 M). Addition was continued until the green color remained. The solid was isolated by filtration followed by washing with THF (2 \times 2 mL) and drying under vacuum. An XPS sample was prepared as described above.

Reaction of [Al(OSiEt₃)₃]₂ with *x* equiv of H₂O/Aluminum. $x = 0.125$: A THF solution (2.0 mL) of [Al(OSiEt₃)₃]₂ (2.078 g, 2.47 mmol) was placed in a preweighed Schlenk flask. To this was added a stock solution of H₂O in THF (0.25 mL, 4.93 M solution, 1.23 mmol). The flask was set aside for 2 weeks at ambient temperatures, after which the volatiles were removed under vacuum (45°C) to yield a waxy white solid: yield 1.852 g.

$x \geq 0.25$: Using the above method [Al(OSiEt₃)₃]₂ was reacted with *x* equiv of H₂O/aluminum, where *x* was increased by 0.125-equiv increments from 0.125 to 1.25 when gelation occurred.

Reaction of [Al(OSiEt₃)₃]₂ with 0.25 equiv of H₂O/Aluminum. [Al(OSiEt₃)₃]₂ (2.00 g, 2.47 mmol) was dissolved in THF (2.0 mL) in a preweighed flask; to this a THF solution of H₂O (0.25 mL, 4.94 M, 1.24 mmol) was subsequently added via syringe. After 5 days, the volatiles were removed in vacuo (10^{-4} Torr) at 35°C until a constant weight was obtained (ca. 48 h). The yield of waxy white solid was 1.94 g and corresponded to complete conversion of the starting materials to a material with an empirical formula of Al(OH)_{0.25}(OSiEt₃)_{2.75}. Anal. Calcd for C₆₆H₁₆₇Al₄O₁₂Si₁₁: C, 50.53; H, 10.66. Found: C, 50.38; H, 10.59. XPS atomic ratios; Al, 4.0; O, 11.9; Si, 11.0. IR (cm⁻¹): 3662 (m, $\nu(\text{OH})$), 2954 (s), 2910 (s), 2876 (s), 2807 (w), 2731 (w), 1594 (m), (OH, bend), 1459 (s), 1414 (s), 1378 (w), 1238 (s, Si-C), 1066 (vs, br, Si-O), 1016 (vs, Si-O), 967 (vs, Si-O), 810 (vs, Al-O), 762 (s, Al-O), 688 (vs, Al-O), 668 (m), 637 (s), 585 (s), 551 (s), 501 (w). NMR (CDCl₃): ^1H , 1.14 [t, $J(\text{H-H}) = 7.9$ Hz, CH₂CH₃], 1.04 [t, $J(\text{H-H}) = 7.2$ Hz, CH₂CH₃], 0.94 [t, $J(\text{H-H}) = 7.9$ Hz, CH₂CH₃], 0.76 [q, $J(\text{H-H}) = 7.9$ Hz, CH₂CH₃], 0.48 [q, $J(\text{H-H}) = 7.9$ Hz, CH₂CH₃]; ^{13}C , 7.76 (CH₂CH₃ and CH₂CH₃), 7.08 (CH₂CH₃), 6.48 (CH₂CH₃), 6.16 (CH₂CH₃).

Reaction of [Al(OSiEt₃)₃]₂ with 0.25 equiv of D₂O/Aluminum. The same procedure was followed as above, with the substitution of D₂O for H₂O. The yield was 1.93 g. ^2H NMR (C₆H₆): 3.1 (1 H, $W_{1/2} = 32$ Hz), 1.32 (2 H, $W_{1/2} = 15$ Hz).

Al₁₀(OH)₁₆(OSiEt₃)₁₄ (6). A weighed amount (1.94 g, 1.24 mmol) of the alumoxane having the empirical formula of Al₄(OH)(OSiEt₃)₁₁, from the procedure outlined above, was heated in vacuo (10^{-4} Torr) at 80°C until constant weight was achieved (ca. 3 days). The white, powdery residue (0.27 g) was dissolved in pentane: benzene (3 mL, 40:60). Cooling the resulting solution to -10°C yielded large, colorless, hexagonal-shaped crystals of Al₁₀(OH)₁₆(OSiEt₃)₁₄ (0.17 g, 0.071 mmol, 92%). Anal. Calcd for C₈₄H₂₂₆Al₁₀O₃₀Si₁₄: C, 42.40; H, 9.57. Found: C, 42.15; H, 9.65.

Table VI. Summary of X-ray Diffraction Data for $\text{Al}_{10}(\text{OH})_{16}(\text{OSiEt}_3)_{14}$ (6)

formula	$\text{C}_{84}\text{H}_{226}\text{Al}_{10}\text{O}_{30}\text{Si}_{14}$
space group	$P\bar{1}$
a , Å	15.62 (1)
b , Å	15.92 (2)
c , Å	17.768 (7)
α , deg	106.84 (7)
β , deg	97.56 (5)
γ , deg	119.33 (6)
V , Å ³	3485 (4)
Z	1
$D(\text{calcd})$, g/cm ³	1.134
cryst dimens, mm	$0.41 \times 0.42 \times 0.38$
temp, K	273 (graphite monochromator)
radiation	Mo $K\alpha$ 0.710 73 Å
μ , cm ⁻¹	2.43
2θ limits	4.0–40.0
scan type	ω
no. of data collected	6650
no. of unique data	6313
no. of obsd data	4305 [$F > 2.0\sigma(F)$]
R	0.125
R_w	0.143
GOF	1.36
final residual, e Å ⁻³	0.68

IR (cm⁻¹): 3708 (w, $\nu(\text{OH})$), 3660 (w, $\nu(\text{OH})$), 3583 (w, $\nu(\text{OH})$), 2956 (vs), 2912 (s), 2878 (s), 1597 (w, O–H bend), 1460 (m), 1414 (m), 1379 (w), 1343 (w), 1304 (w), 1239 (m, Si–C), 1153 (w), 1056 (vs, Si–O), 1015 (s, Si–O), 965 (vs, Si–O), 738 (vs, Al–O), 660 (s, Al–O), 630 (s), 575 (m), 474 (w).

$\text{Al}_{10}(\text{OD})_{16}(\text{OSiEt}_3)_{14}$. The same procedure was followed as above, with the substitution of $\text{Al}_4(\text{OD})(\text{OSiEt}_3)_{11}$ for $\text{Al}_4(\text{OH})(\text{OSiEt}_3)_{11}$. The yield was 0.18 g. NMR (C_6H_6): ²H 6.8 (2D), 4.6 (2D), 3.7 (2D), 2.1 (8D), 0.84 (2D), see text for assignment.

X-ray Crystallographic Study. A crystal data summary is given in Table VI; fractional atomic coordinates of all Al, Si, and O atoms are given in Table VII.

The crystals of 6 were highly solvent dependent, removal from the mother liquor caused the crystal to powder within seconds, while attempts to cool the crystal below ambient temperatures resulted in cracking. The crystals were therefore sealed in a glass capillary along with a quantity of the supernatant from their crystallization. Under these conditions, although poorly diffracting, no deterioration of the crystal was observed during the data collection.

X-ray diffraction data were collected on a Nicolet R3m/V four circle diffractometer. Data collection was controlled with the Nicolet P3 program.⁴⁸ The unit cell was indexed by using 20 reflections obtained from a rotation photograph. A lattice determination using both the P3 program and XCELL suggested a triclinic cell. This was confirmed by the lack of any systematic extinction or any diffraction symmetry other than the Friedel conditions. The two possible triclinic space groups are the noncentrosymmetric $P1$ [C_1 ; No. 1] or the centrosymmetric $P\bar{1}$ [C_1 ; No. 2]. With $Z = 1$ and no expectation of a chiral molecule, the latter centrosymmetric space group would seem more probable and was later found to be the correct choice (see below). The final unit cell parameters were obtained by a least-squares refinement of 30 selected reflections in the range $10^\circ < 2\theta < 30^\circ$.

A total of 6650 reflections were collected in the range $4^\circ < 2\theta < 40^\circ$. Of these 6313 were unique reflections and 4305 with $F_o > 2\sigma(F_o)$ were used in the structure solution. The intensities of three check reflections were measured every 60 reflections; the intensities did not vary significantly during the data collection. Lorentz and polarization corrections were applied to the data. The SHELXTL-PLUS series programs⁴⁹ was used for all calculations.

Initial attempts to solve the structure in $P\bar{1}$ did not provide a chemically reasonable result. However, all of the aluminum, oxygen and silicon atom positions were readily revealed in $P1$ by the use of direct methods. From this initial solution it is clear

Table VII. Selected^a Atomic Coordinates ($\times 10^4$) and Equivalent Isotropic Displacement Coefficients ($\text{Å}^2 \times 10^3$)^b for $\text{Al}_{10}(\text{OH})_{16}(\text{OSiEt}_3)_{14}$ (6)

	x	y	z	$U(\text{eq})$
Al(1)	4026 (3)	4944 (3)	5121 (2)	34 (2)
Al(2)	3951 (3)	3474 (3)	3578 (2)	34 (3)
Al(3)	2072 (3)	3838 (3)	3470 (3)	42 (3)
Al(4)	5818 (3)	5020 (3)	3034 (3)	42 (3)
Al(5)	3728 (3)	1325 (3)	2429 (3)	43 (3)
Si(31)	200 (4)	2000 (5)	3773 (4)	97 (4)
Si(32)	791 (4)	4410 (4)	2373 (3)	68 (3)
Si(41)	7314 (4)	5261 (5)	1884 (3)	75 (3)
Si(42)	5282 (5)	6748 (4)	3037 (4)	78 (4)
Si(51)	1975 (5)	-1146 (4)	1953 (4)	88 (4)
Si(52)	5774 (4)	1562 (4)	3347 (3)	67 (4)
Si(53)	3393 (4)	1468 (4)	683 (3)	70 (3)
O(121)	4779 (6)	4994 (7)	4305 (5)	35 (5)
O(12)	3357 (6)	3545 (6)	4427 (5)	35 (5)
O(21)	5100 (6)	3640 (7)	4282 (5)	36 (5)
O(13)	2980 (7)	4946 (7)	4474 (5)	41 (6)
O(23)	2915 (7)	3572 (7)	3001 (5)	43 (6)
O(14)	6560 (7)	5311 (7)	4057 (5)	41 (6)
O(24)	4652 (7)	3769 (7)	2804 (5)	41 (5)
O(25)	3268 (7)	2048 (7)	3039 (5)	41 (6)
O(31)	1150 (7)	2785 (8)	3589 (6)	61 (7)
O(32)	1676 (8)	4388 (8)	2936 (6)	65 (7)
O(41)	6468 (8)	4978 (8)	2355 (6)	59 (7)
O(42)	5499 (8)	5887 (8)	3250 (6)	50 (6)
O(51)	2832 (8)	3 (8)	2063 (6)	65 (7)
O(52)	4915 (7)	1830 (7)	3140 (6)	50 (6)
O(53)	3908 (8)	1826 (7)	1672 (5)	50 (6)

^a For C atomic positions see supplementary material.

^b Equivalent isotropic $U(\text{eq})$ defined as one-third of the trace of the orthogonalized U_{ij} tensor.

that the Al_{10} core is centrosymmetric, so the solution was transformed from $P1$ to $P\bar{1}$, and the successful refinement of the structure in the latter space group thus resulted.

Standard difference map techniques were used to find all of the remaining non-hydrogen atoms. Due to difficulties in refining four of the ethyl groups the carbon positions were constrained by the use of DFIX cards, for which the C_α – C_β distances were allowed to refine freely using a FVAR card for each ethyl. The final DFIX values were based on these refined FVAR values. All 138 non-hydrogen atoms were located and refined anisotropically. Subsequent difference maps revealed some but not all of the hydrogens bound to the core oxygens, but chemical charge balance considerations dictated that all the oxygens bridging Al atoms be hydroxide groups. Therefore, all hydroxide hydrogens were included by using a riding model [$d(\text{O–H}) = 1.02$ Å; $U_{\text{iso}}(\text{H}) = 1.2U_{\text{iso}}(\text{O})$]. The hydrogen atoms associated with the ethyl groups were placed in calculated positions [$d(\text{C–H}) = 0.96$ Å; $U_{\text{iso}}(\text{H}) = 1.2U_{\text{iso}}(\text{C})$] for refinement. Refinement was performed to convergence ($\Delta/\sigma(\text{max}) < 0.01$) with this model. The weighting scheme was $w^{-1} = \sigma^2(F) + 0.0095F^2$. The final difference map was essentially featureless with all peaks less than 0.68 e Å⁻³. Duplicate attempts at data collection and structural refinement were undertaken but with no overall improvement.

Despite the location and refinement of all the non-hydrogen atoms the R factor of 0.125 and the high esd's for some bond distances and angles could not be further reduced. This is undoubtedly due to both the high thermal motion associated with the 273 K data collection and the "light atom" nature of the structure. However, since all the chemically equivalent structural parameters are within experimental error of each other and most importantly previously reported values, and the structure is wholly consistent with the NMR spectroscopic data, this solution is undoubtedly correct. In addition, since only atom connectivity is important in the present case we do not believe the high esd's and R factors detract from the overall result.

Acknowledgment. Financial support for this work is provided by the Aluminum Research Board, Dr. R. P. Tooze at ICI, Wilton Materials Research Centre (UK), and Dr. K. Wynne at the Office of Naval Research. We thank the NSERC (Canada) for a postdoctoral fellowship (A. W.A.). Dr. A. P. Sattelberger, Isotope and Nuclear

(48) P3/R3 Data Collection Manual; Nicolet Instrument Corp.: Madison, WI, 1987.

(49) SHELXTL-PLUS Users Manual; Nicolet Instrument Corp.: Madison, WI, 1988.

Chemistry Division, Los Alamos National Laboratory, is gratefully acknowledged for the gift of ^{17}O -enriched water. We are indebted to Dr. Andrew N. MacInnes for assistance with the XPS measurements and Ms. Susan Bradley for the artwork in Figure 10.

Registry No. 6, 137570-63-9; I, 135604-10-3; II (L = THF), 137570-61-7; II (L = 4-MePy), 137570-62-8; AlMe₃, 75-24-1; ^{29}Si ,

14304-87-1; ^{17}O , 13968-48-4; boehmite, 1318-23-6; alumina, 1344-28-1; aluminum silicate, 1335-30-4.

Supplementary Material Available: Full listings of bond lengths and angles, anisotropic thermal parameters, and hydrogen atom parameters (8 pages); tables of calculated and observed structure factors (23 pages). Ordering information is given on any current masthead page.

Proton Spin-Lattice Relaxation in the Rotating Frame Measurements for Some Industrial Polyethylene Composites

A. Natansohn

Department of Chemistry, Queen's University, Kingston, Ontario, K7L 3N6 Canada

Received July 29, 1991. Revised Manuscript Received October 9, 1991

Proton spin-lattice relaxation time in the rotating frame is measured for two polyethylene (PE) samples and a few of their composite materials with CaCO₃ and a cellulosic filler. The composites with poorer impact properties have detectable quantities of monoclinic PE crystals. Each material has a different relaxation behavior. While it is difficult to draw conclusions from the differences in the relaxation of the main signal of PE, the analysis of the amorphous signal relaxation suggests that there are at least two kinds of amorphous domains of PE. The presence of a faster relaxing, higher in proton density and/or mobility, amorphous domain can be associated with improved impact properties of the composite.

Introduction

Since high-resolution solid-state ^{13}C NMR spectroscopy was first proposed in 1976,¹ polyethylene (PE) has probably been one of the most investigated polymers using this method. It is well established now that the two main peaks appearing in the spectrum of almost any PE sample are assignable to the amorphous domains (the broader higher field peak at ca. 31 ppm) and to a mixture of crystalline, amorphous, and maybe "interfacial" domains (the main peak at 32.8 ppm). A considerable effort has been directed to measurement and interpretation of $T_1(\text{C})$ (carbon spin-lattice relaxation time) values. Very recent data are summarized in a review on the subject.²

Apart from $T_1(\text{C})$, the existence of a mixture of crystalline and amorphous domains was proven by measuring some other relaxation parameters. $T_1(\text{H})$ (proton spin-lattice relaxation time) and $T_{1\rho}(\text{H})$ (proton spin-lattice relaxation time in the rotating frame) reflect bulk properties, because protons are abundant spins and the magnetization is easily transmitted within various domains.³ Both parameters were investigated by Packer⁴ and found to be different for different domains within the sample. This was expected, because it is well-known that both these parameters can be used as probes for the phase structure of multiphase systems.³ The use of $T_{1\rho}(\text{H})$ as a probe for polymer blend miscibility was first suggested in 1981.⁵ Another parameter measured in various PE samples is T_{CH} , the cross polarization time. Its value is related to the ease with which magnetization is transmitted from protons to carbons. An inversion-recovery pulse

sequence has been applied by Ritchey et al.⁶ Data for low-density polyethylene, together with data for other polymers, seem to show a correlation with the dynamic storage modulus, an important property for polymers used as materials.⁷ Finally, the last parameter measured on PE is T_{DD} , the time constant for the decay of protonated carbon signals in the absence of cross polarization.⁸

All these parameters indicate the complicated phase structure of various polyethylenes. While every one of them shows different values for crystalline and amorphous regions, in some instances more information can be obtained from the spectra. Biexponential decays were observed for both amorphous and crystalline domains in measuring T_{DD} .⁸ The existence of an intermediary, interfacial layer in PE samples was postulated by Kitamaru et al.,⁹ who analyzed the ^{13}C CP-MAS NMR spectra using a broad resonance at 31.3 ppm assignable to interfacial domains. This finding was recently confirmed by Packer et al.¹⁰ in an indirect way. They used the carbon spectrum to measure $T_{1\rho}(\text{H})$ for every 0.1 ppm within the PE signal. The analysis was performed in terms of a biexponential decay, and a certain region within the main signal was found to have an increased amount of the fast decaying species (amorphous components). This area was assigned to the interfacial domain, in analogy with Kitamaru's results. Another significant publication identified α , β , γ , δ , ϵ , ζ , η , θ , ι , κ , λ , μ , ν , ξ , \omicron , π , ρ , σ , τ , υ , ϕ , χ , ψ , ω , α , β , γ , δ , ϵ , ζ , η , θ , ι , κ , λ , μ , ν , ξ , \omicron , π , ρ , σ , τ , υ , ϕ , χ , ψ , ω rhombic and monoclinic signals of as-produced PE.¹¹

(1) Schaefer, J.; Stejskal, E. O. *J. Am. Chem. Soc.* 1976, 98, 1031.

(2) Laupretre, F. *Prog. Polym. Sci.* 1990, 15, 425.

(3) VanderHart, D. L. *Makromol. Chem., Macromol. Symp.* 1990, 34, 125.

(4) Packer, K. J.; Pope, J. M.; Yeung, R. R.; Cudby, M. E. A. *J. Polym. Sci., Polym. Phys. Ed.* 1984, 22, 589.

(5) Stejskal, E. O.; Schaefer, J.; Sefcik, M. D.; McKay, R. A. *Macromolecules* 1981, 14, 275.

(6) Parker, A. A.; Marcinko, J. J.; Shieh, Y. T.; Shields, C.; Hedrick, D. P.; Ritchey, W. M. *Polym. Bull.* 1989, 21, 229.

(7) Parker, A. A.; Marcinko, J. J.; Shieh, Y. T.; Hedrick, D. P.; Ritchey, W. W. *J. Appl. Polym. Sci.* 1990, 40, 1717.

(8) Cholli, A. L.; Ritchey, W. M.; Koening, J. L.; Veeman, W. S. *Spectrosc. Lett.* 1988, 21, 519.

(9) Kitamaru, R.; Horii, F.; Murayama, K. *Macromolecules* 1986, 19, 636.

(10) Packer, K. J.; Poplett, I. J. F.; Taylor, M. J.; Vickers, M. E.; Whittaker, A. K.; Williams, K. P. *J. Makromol. Chem., Macromol. Symp.* 1990, 34, 161.

(11) Jarrett, W. L.; Mathias, L. J.; Porter, R. S. *Macromolecules* 1990, 23, 5164.